ELASTIC-PLASTIC BUCKLING OF INFINITELY LONG PLATES RESTING ON TENSIONLESS FOUNDATIONS

by

Yongchang Yang

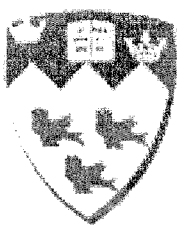

Department of Civil Engineering and Applied Mechanics

McGill University

Montreal, Quebec, Canada

April 2007

A thesis submitted to the Graduate and Postdoctoral Studies Office
in partial fulfilment of the requirements of the degree of
Master of Engineering

Your file Votre référence
ISBN: 978-0-494-38497-8
Our file Notre référence
ISBN: 978-0-494-38497-8

Abstract

There is a class of plate buckling problems in which buckling occurs in the presence of a constraining medium. This type of buckling has been investigated by many researchers, mainly as buckling of elastic columns and plates on elastic foundations. Analytical solutions have been obtained by assuming the foundation to provide tensile as well as compressive reaction forces. The present work differs from the previous ones in two respects. One, the foundation is assumed to be one-sided, thus providing only the compressive resistance. Two, the plates are allowed to be stressed in the plastic, strain-hardening range. Equations for determining the buckling stresses and wavelengths are obtained by solving the differential equations for simply supported and clamped long rectangular plates stressed uniformly in the longitudinal direction. The relevance and the usefulness of the obtained formulas is demonstrated by comparing the predicted results with the experimental results of other researchers on buckling of concrete filled steel box-section and HSS columns. It is shown that the theoretical buckling loads match quite closely with the experimental ones, and hence, should prove useful in formulating rules for the design of such columns.

Résumé

Il y a une catégorie de problèmes liés au voilement des plaques minces dans lesquels le flambage se produit en présence d'un milieu de contrainte. Ce type de flambage a été considérablement étudié par les chercheurs comme étant un problème de flambage de colonnes et des plaques élastiques sur fondation élastique. Des solutions analytiques ont été obtenues en supposant que la fondation fournit de forces de réaction compressives aussi bien que de tension. Le travail actuel diffère du précédent à deux égards. Premièrement, on suppose que la fondation ne peut fournir que des réactions compressives. Deuxièmement, les plaques sont sollicitées dans le domaine post-élastique. Des formules pour les charges de flambage et les longueurs d'onde décrivant les modes de flambage sont obtenues, en résolvant les équations différentielles pour les cas des plaques longues rectangulaires soumises à un effort uniforme en direction longitudinale. La pertinence et l'utilité des formules obtenues sont démontrées en comparant les résultats prédits avec des résultats expérimentaux obtenus par d'autres chercheurs pour le flambage de tubes rectangulaires en acier remplis de béton et des colonnes tubulaires de type HSS. On remarque que les prédictions du flambage théorique sont très similaires aux résultats expérimentaux. En conséquence, le modèle théorique devrait s'avérer utile pour formuler des règles pour la conception de colonnes de ce type.

Acknowledgments

I would like to express sincere thanks to my research supervisor Professor S. C. Shrivastava of Department of Civil Engineering and Applied Mechanics, McGill University, whose help, stimulating suggestions, and encouragement helped me at all times in doing the research and writing this thesis.

I would like to express special thanks to my wife Weixia, whose love, patience, and unwavering support enabled me to complete this work.

Table of Contents

Abstract i
Resume (French) ii
Acknowledgments iii
Table of Contents iv
List of Major Symbols vi
List of Figures viii
List of Tables x

Chapter 1 Introduction 1

1.1 Definition of the problem 1
1.2 Literature review 6
1.3 Statement of the objectives 9

Chapter 2 Elastic Buckling of Infinitely Long Plates on Elastic Foundations 10

2.1 Governing equations of equilibrium 10
2.2 Buckling deflections in contact and no-contact zones 17
2.2.1 Solution for buckling deflections in contact zones 17
2.2.2 Solution for buckling deflections in no-contact zones 19
2.3 Matching conditions between contact and no-contact regions 21
2.4 Equations for buckling loads and wavelengths by the equilibrium method 23
2.5 Equations for buckling loads and wavelengths by the method of virtual work 25
2.6 Solutions of buckling loads and wavelengths under simply supported edges ... 29
2.7 Solutions of buckling loads and wavelengths under clamped edges 33

Chapter 3 Plastic Buckling of Infinitely Long Plates Resting on Elastic Foundations 36

3.1 Constitutive relations of the plasticity theories 36
3.2 Constitutive relations for a plastic bifurcation analysis 39
3.3 Equations for buckling loads and wavelengths by the equilibrium method 41

3.3.1 Equations for buckling displacements in the contact and no-contact regions 42
3.3.2 Derivation of the buckling equations 43
3.4 Equations for buckling loads and wavelengths by the method of virtual work 44
3.5 Buckling loads and wavelengths for simply supported plates 45
3.6 Buckling loads and wavelengths for clamped plates 50

Chapter 4 Application to Concrete-filled Steel Box Columns, and Verifications with Experiments 53

4.1 Application to concrete-filled steel box columns 53
4.2 Verification with experiments 57

Chapter 5 Summary and Conclusions 66

5.1 Summary 66
5.2 Conclusions 69
5.3 Suggestions for future work 69

References 71

List of Major Symbols

a	plate length
b	plate width
A_c, A_s	area of concrete core, area of steel section
$\overline{B}$, $\overline{C}$, $\overline{D}$, $\overline{F}$	general moduli for plate buckling analysis
B',C',D', F'	elastic-plastic moduli in plastic plate buckling
c_1, d_1	related to roots of the characteristic equation in the contact part
c_2, d_2	related to roots of the characteristic equation in the no-contact part
e, g	parameters in elastic-plastic moduli, $e = E/E_s - 1$, $g = E/E_t$
D	elastic rigidity of a plate
E	Young's modulus of elasticity
E_t	tangent modulus
E_s	secant modulus
J_2	second invariant of the deviatoric stress s_{ij}, $J_2 = \frac{1}{2}s_{ij}s_{ij}$
$f_c^{'}$	crushing strength of concrete in cylinder test
G	shear modulus
k	modulus of elastic foundation
M_{xx}, M_{yy}, M_{xy}	moment stress resultants per unit length
N_{cr}	buckling load per unit length ($= \sigma_{cr}\, t$)
N_c	ultimate strength of concrete core ($= 0.85 f_c^{'} A_c$)
N_s	bifurcation load of the steel section of the column ($= \sigma_{cr} A_s$)
N_T	the capacity predicted by the present theory for the column
N_u	the capacity obtained in experiments for the box columna
s_{ij}	deviatoric stress components, $s_{ij} = \sigma_{ij} - \frac{1}{3}\sigma_{kk}\delta_{ij}$
t	plate thickness
$w_1(x_1, y)$, $w_2(x_2, y)$	buckling deflections in contact and no-contact regions
x, y, z	coordinate directions
α	foundation modulus parameter ($= kb^4/\pi^4 D$)
Γ_1, Γ_2, Γ_1', Γ_2'	coefficients of differential equations in contact and no-contact zones elastic buckling of simply supported plates
$\overline{\Gamma}_1$, $\overline{\Gamma}_2$, $\overline{\Gamma}_1'$, $\overline{\Gamma}_2'$	coefficients of differential equations in contact and no-contact zones elastic buckling of clamped plates

$\Gamma_3, \Gamma_4, \Gamma'_3, \Gamma'_4$	coefficients of differential equations in contact and no-contact zones plastic buckling of simply supported plates
$\overline{\Gamma}_3, \overline{\Gamma}_4, \overline{\Gamma}'_3, \overline{\Gamma}'_4$	coefficients of differential equations in contact and no-contact zones plastic buckling of clamped plates
$\epsilon_{xx}, \epsilon_{yy}, \epsilon_{xy}$	plate strains due to buckling, ϵ_{ij}
$\phi_1(x_1)$	buckling function in x direction, contact part $x = x_1$
$\phi_2(x_2)$	buckling function in x direction, no-contact part $x = x_2$
$\psi(y)$	buckling function in y direction
λ	buckling load parameter for a plate ($= N_{cr}b^2 / \pi^2 D$)
μ	$\mu = \pi/b$
ν	Poisson's ratio
$\sigma_{xx}, \sigma_y, \sigma_{xy}$	plate stresses due to buckling, σ_{ij}
σ_e	von Mises equivalent stress, $\sigma_e = \sqrt{3J_2} = \sqrt{\frac{3}{2}s_{ij}s_{ij}}$
σ_Y	yield stress of steel
$2\zeta, 2\xi$	buckle lengths, contact and no-contact parts

List of Figures

Figure 1-1 Concrete-filled steel box section column [1] 2
Figure 1-2 Delamination in a composite plate - buckling mode 2
Figure 1-3 Buckling modes of short plates 3
Figure 1-4 Buckling mode of an infinitely long plate resting on a one-way elastic foundation, showing zones of contact and no-contact 4

Figure 2-1 Buckling mode of an infinitely long plate constrained unilaterally by an elastic foundation 11
Figure 2-2 Forces and moments acting on a plate coordinate element 11
Figure 2-3 Longitudinal section of buckling mode of an infinitely long plate resting on a one-way elastic foundation 16
Figure 2-4 Buckling load coefficient - foundation stiffness parameter curves with different boundary conditions 31
Figure 2-5 Wavelength to width ratio - foundation stiffness parameter curves with simply supported unloaded edges 32
Figure 2-6 Elastic buckling mode of an infinite plate resting on a rigid foundation 32
Figure 2-7 Wavelength to width ratio - foundation stiffness parameter curves with clamped edges 35

Figure 3-1 Uniaxial stress-strain curve for aluminum alloy 24S - T3 46
Figure 3-2 Plastic buckling parameter λ vs. foundation stiffness α for simply supported plates 48
Figure 3-3 Contact length /plate-width vs. foundation stiffness for simply supported plates; Deformation theory results 49
Figure 3-4 Contact length /plate-width vs. foundation stiffness for simply supported plates; Incremental theory results 49
Figure 3-5 Plastic buckling parameter λ vs. foundation stiffness α for clamped plates 51
Figure 3-6 Contact length /plate-width vs. foundation stiffness for clamped plates; Deformation theory results 52
Figure 3-7 Contact length /plate-width vs. foundation stiffness for clamped plates; Incremental theory results 52

Figure 4-1 Typical failure modes of concrete-filled box columns [1] 54
Figure 4-2 Sections of steel box columns 55
Figure 4-3 Buckling mode sections of steel box columns 56
Figure 4-4 Buckling load coefficient λ_{cr} vs. aspect ratio a/b for simply supported isotropic elastic plates fixed to a foundation of stiffness α [4] 57
Figure 4-5 Ramberg- Osgood curve of steel ($\sigma_y = 281$MPa) used in the experiments conducted by Liang and Uy [5] 58
Figure 4-6 Ramberg-Osgood curve for steel used in the experiment conducted by Uy [6] 59
Figure 4-7 Ramberg-Osgood curve for steel used in the experiment conducted by D. Liu *et al.* [1] 59
Figure 4-8 Scatter for the present theoretical predictions vs. experiments in [5] 64
Figure 4-9 Scatter for the present theoretical predictions vs. experiments in [6] 64
Figure 4-10 Scatters for the present theory, EC4, AISC, and ACI vs. experiments in [1] 65

List of Tables

Table 2.1 λ, ζ and ξ for elastic infinitely long simply supported plates resting on different tensionless foundations 30

Table 2.2 λ, ζ and ξ for elastic infinitely long, clamped plates resting on different tensionless foundations 34

Table 3.1 λ, ζ and ξ for an infinitely long simply supported Al alloy 24S - T3 plate resting on elastic one-way foundations with different foundation parameter α ($b/t = 25$, Deformation theory) 47

Table 3.2 λ, ζ and ξ for an infinitely long, simply supported Al alloy 24S - T3 plate resting on elastic one-way foundations with different foundation parameter α ($b/t = 25$, Incremental theory) 47

Table 3.3 λ, ζ, ξ for an infinitely long, clamped Al alloy 24S-T3 plate resting on one-way elastic foundations for different foundation parameter α ($b/t = 25$, Deformation theory) 50

Table 3.4 λ, ζ, ξ for an infinitely long, clamped Al alloy 24S-T3 plate resting on one-way elastic foundations for different foundation parameter α ($b/t = 25$, Incremental theory) 50

Table 4.1 Comparison of the present theoretical predictions N_T with experiments 62

Table 4.2 Comparison of the present theoretical predictions N_T with experiments 62

Table 4.3 Geometric and material properties of test specimens [1] 63

Table 4.4 Comparison of the present theoretical predictions N_T with experimental results [1], EC 4, AISC, and ACI 63

Chapter 1

Introduction

1.1 Definition of the problem

There are a number of problems dealing with the buckling of columns, plates, and shells in which buckling takes place in the presence of a constraining (solid or fluid) medium. The well-known examples are buckling of columns and plates against elastic foundations. Generally, it is assumed that the structure is bonded to the foundation and the foundation can provide tensile as well as compressive forces of resistance. Such problems are termed as buckling of structures on two-way foundations. In contrast to this situation, the problems of buckling in which the structure is not bonded to the foundation, and thus the foundation only provides compressive resistance, are termed as one-way buckling problems. This latter category of problems is more difficult to analyze. The present work falls into this latter category.

Concrete-filled box columns fabricated with steel plates, Fig. 1-1, or concrete-filled large HSS columns, have been used increasingly in building construction, especially in high-rise buildings, in recent years. They provide the advantages of high strength, high ductility, large strain capacity, and reduction in construction costs. These advantages are typical of such composite structures. Neglecting the weak bond which might exist between the steel and concrete interfaces, the steel plates in the concrete-filled box column are constrained by the concrete only against their inward movement. The resistance to (one-way) buckling of such columns is increased considerably over those without the concrete filling. The buckling when it occurs, is localized, as shown in Fig. 1-1(c), Reference [1].

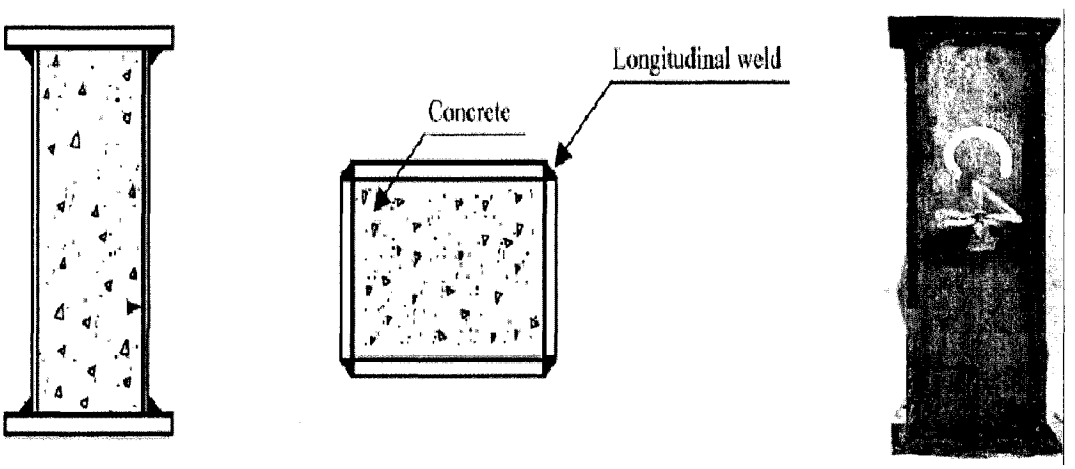

(a) Elevation view (b) Plan view (c) Failure mode

Fig. 1-1 Concrete-filled steel box section column [1]

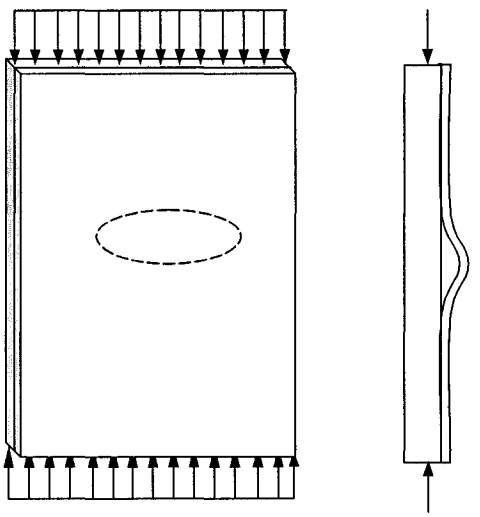

Fig. 1-2 Delamination in a composite plate - buckling mode

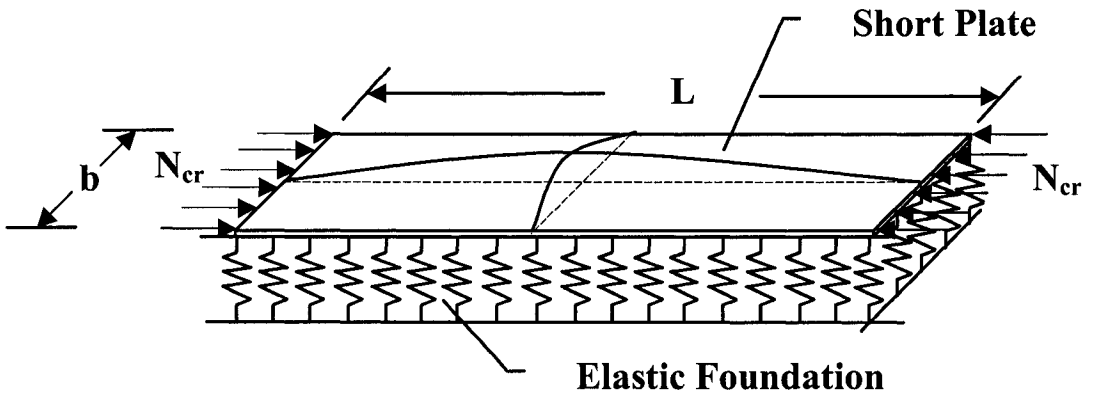

(a) Lift-up buckling mode

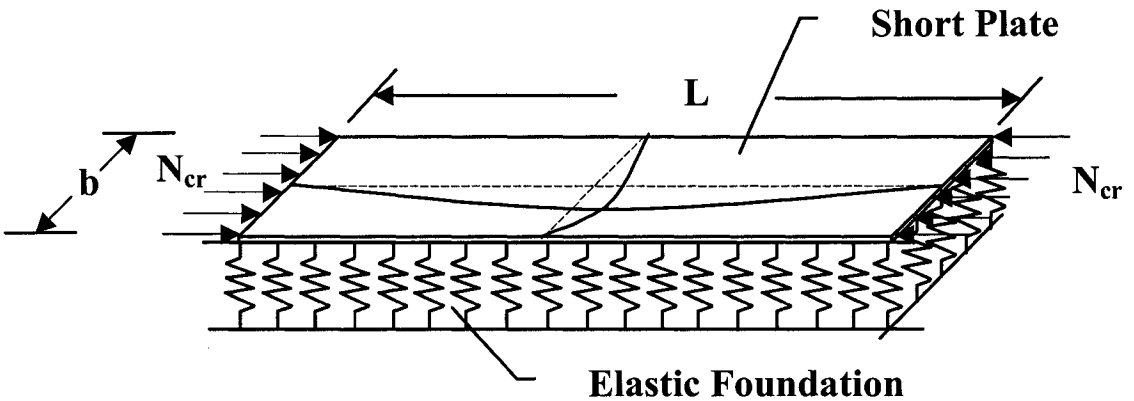

(b) Downward buckling mode

Fig. 1-3 Buckling modes of short plates

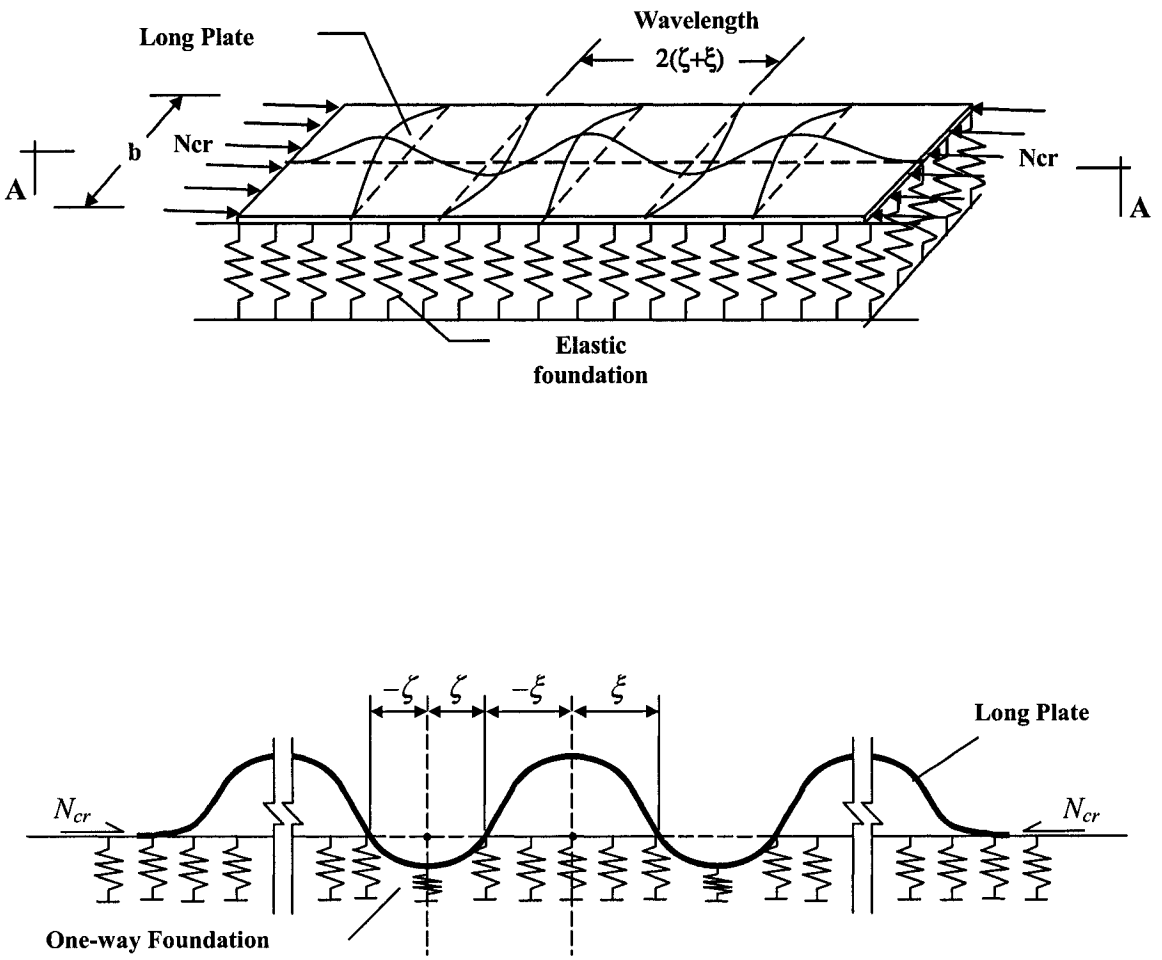

Section A-A

Fig. 1-4 Buckling mode of an infinitely long plate resting on a one-way elastic foundation, showing zones of contact and no-contact

The phenomenon of "lift-off" of welded railway tracks due to constrained thermal expansion is well known. Relevant studies [2, 3] have shown this to be a one-way buckling problem in which the foundation is unable to restrain the upward buckling of the railway track. The temperature induced 'pop-up' of a pipeline in the vertical plane is another example of one-way buckling problems.

The interlaminar matrix delamination, Fig. 1-2, encountered frequently in composite materials, such as FRP (Fibre reinforced polymer) composites, can also be considered as a one-way buckling problem. That this is an important issue is evident from the numerous experimental and analytical investigations reported in the current literature [2, 3, 4]. Surface delamination in composites can also be thought of as a one-way plate buckling on account of bond failure from the larger substrate. The substrate acts as a one-sided constraint on the surface delamination layer.

The above stated and other relevant problems have driven the interests of many researchers. They are generally treated as stability problems of a plate or a column, with or without the consideration of self-weight, subjected to compressive loads and resting on elastic foundations, Figs. 1-3 and 1- 4.

To seek solutions for this class of problem, a number of methodologies have been reported in the literature. Some researchers [5, 6, 7] have used the finite element and finite strip methods. The approximate numerical results thus found have usually proved to be of real, but limited, value. In many of these studies, the foundation was regarded as capable of providing both compressive as well as tensile reactions, despite the fact that this assumption may not have been a realistic one.

The two types of assumptions regarding the foundation action lead to widely differing results. There are only few studies which have dealt with cases in which, although the foundation is elastic, the buckling of the overlying structure may take place in the plastic range. To the best of the author's knowledge, there are no exact solutions dealing with the plastic buckling of plates constrained by tensionless elastic foundations. This problem is obviously important for concrete-filled HSS or steel box columns, as plastic buckling is a more desirable mode of failure than elastic buckling. Therefore, the present work deals with determining exact analytical solutions useful for both elastic and plastic ranges of behaviour. The theoretical problem is that of a thin infinitely long plate resting on a

tensionless elastic foundation, and subjected to uniform compressive forces in the longitudinal direction.

When a plate is supported on foundations that are tensionless, the buckling mode can be of one sign (lift-up or down, Fig. 1-3) or multi-sign having several waves (Fig. 1-4). The former mode is possible for short plates, and the situation can be analyzed by the classical plate buckling theory. If, however, the plate is long, the situation is completely changed. In this latter case there exists the possibility that, under certain compressive forces, regions of contact and no-contact would develop simultaneously. Within the no-contact regions, the plate lifts away from the foundation, and no forces exist between the plate and the foundation. In the contact parts, the plate elicits reaction forces from the foundation. The analysis required to find the equations for such buckling is quite difficult because, in a sense, a nonlinear eigenvalue problem is to be solved. The analysis is further complicated by virtue of the fact that strain-hardening plastic behaviour of the plate material is allowed to occur. The results from the analysis are useful for both elastic and post-elastic i.e., plastic ranges of behaviour. For the latter case, usually treated in an ad hoc fashion, the present analysis furnishes a rational basis for computing the column capacity against buckling. As mentioned before, of special interest is the design of concrete-filled steel box and HSS columns against buckling.

1.2 Literature review

Although there are many studies on elastic buckling of plates on elastic foundations, there are only a few dealing with plastic buckling of plates, and none on plastic buckling of plates on tensionless foundations. Timoshenko [8] was one of the first authors to analyze deflection (not buckling) of rectangular plates subjected to transverse loads, and resting on elastic subgrades. A theory of plastic buckling with its application to geophysics was formulated by Bijlaard [9] in 1938. Bijlaard [10] applied the well-known plasticity theories and obtained bifurcation stresses for axially stressed plates. However, the substratum in Bijlaard's paper was taken to be providing both tensile and compressive reactions. The formulas for buckling loads of elastic plates resting on elastic foundations, were also derived in the book by V. Z. Vlasov and N. N. Leont'ev [11], but again for two-way foundations.

In all the works mentioned above the foundation was assumed to provide two-way resistance equally. Evidently, as pointed out before, this may not always be an acceptable physical situation. Some early researchers did try to address the problem of one-way contact in a different context. Weitsman [12] determined the radius of contact between an infinite elastic plate and a tensionless semi-infinite elastic half space when the plate is subjected to a concentrated transverse force against the half space. The problem was further investigated by Weitsman [13] who determined the displacements in the contact and no-contact regions, but did not discuss stability problems. The displacements of a free rectangular plate resting on a Winkler-type tensionless foundation, subjected to a uniformly distributed load, moment and a concentrated load against the foundation, were obtained by Zekai Celep [14] by addressing the contact and no-contact parts of the plate separately. However, no buckling issue was raised by this author either.

With increasing application of composite materials in 1980's, researchers began to focus on the issue of delamination in composite components. Delamination in laminated plates was addressed by Herzl Chai et al. [3] as a one-way buckling (lift-up) problem, since the supporting sublaminate essentially behaves as a rigid foundation. John Roorda [2] presented, using the energy approach, the essential features of the mechanics of one-way buckling, and examined the growth of buckles and delamination in long, elastic plates, lying on or bonded to a horizontal boundary. However, both of these studies [2, 3] did not specifically address the enhancement of buckling loads from the supporting foundation, as is the case with the present study.

It appears that an analysis of the elastic buckling of infinitely long plates on a one-way elastic foundation was first performed by Paul Seide [15] in 1958. In this study, differential equations of equilibrium were used for the contact and contactless regions, respectively. The bifurcation load was secured by enforcing the matching conditions at the junction of these two regions. This solution assumes all four edges of the plate as simply supported. Subsequently Seide [16] also dealt with plastic buckling of rectangular plates, but on a two-way elastic foundation and using the energy method.

Among recent papers on this subject, it is of special interest to note the work of Khaled Shahwan and Anthony Waas [4, 17]. In these papers, energy methods were employed to analyze the elastic buckling of infinitely long plates on one-way elastic foundations. Exact solutions were obtained for plates simply supported on all four sides. Approximate

solutions were obtained for other cases of support conditions. The novel feature was that the plates were allowed to be of orthotropic elastic material.

As mentioned above, up to the present moment, there are no works which have obtained solutions for the plastic buckling of infinitely long plates resting (i.e., with no bond) on tensionless elastic foundations. The present work obtains these loads by solving the differential equations of equilibrium. The results are exact for the simply supported plates. For clamped plates the differential equations are derived using the method of virtual work and a realistic approximation of the buckle form in the transverse direction, Furthermore, in contrast to the previous works, the theoretical results of the present work have been verified by comparison with experiments.

One of the most relevant applications of the stability theory of plates supported on one-way foundations, is in determining the strength of concrete-filled steel box columns. As mentioned earlier, predicting and testing the capacities of such columns have become increasingly important in recent times due to their use in high-rise construction. Brain Uy et al. have conducted a number of experiments [5, 6, 7] to test the ultimate strengths of hollow as well as concrete-filled box columns of steel. In these researches the theoretical buckling loads (i.e., ultimate strength of steel sections) were found by numerical means namely by the finite strip method. Orthotropic plate behavior and energy methods were used by H. D. Wright [18, 19] to analyze buckling of such columns. Although Wright had considered many different cases of boundary conditions for the plate components of columns, the constraining influence of the concrete in-fill was taken into account only very roughly by adjusting the boundary conditions of the plates.

The current design codes, e.g., Eurocode 4 (EC4), American Institute of Steel Construction (AISC), and American Concrete Institute (ACI), generally determine the axial compressive capacity of concrete-filled steel box columns by summing up the strength of the steel hollow section and of the concrete core. The strength of steel section is computed on the basis of elastic buckling or yield strength of the constituent steel plates of the section and modified by some empirical factors. However, these factors generally ignore the enhancement of the buckling strength of the plates due to the (one-way) constraint provided by the concrete core. Also, some of these codes are not applicable to high strength steel or concrete materials.

1.3 Statement of the objectives

In consideration of the foregoing discussion, the objectives for the present investigation were defined to be:

(i) Derivation of the exact or quasi-exact solutions for the elastic bifurcation buckling of infinitely long plates resting on tensionless elastic foundations, subjected to axially compressive forces in the longitudinal direction. The solutions will consist of determining, by the equilibrium method or the virtual work method, the critical bifurcation loads and the corresponding wavelengths, for plates either simply supported or clamped along the unloaded edges, Fig. 1-4.

(ii) Derivation of the exact or quasi-exact solutions for the plastic bifurcation buckling of the same class of plates stated above in (i) and shown in Fig. 1-4, by employing the constitutive relations of both the deformation and the incremental theories of plasticity, and by using the equilibrium method or the virtual work method of analysis.

(iii) Application of the analytical results to concrete-filled steel box columns, and their verification by comparison with experimental results, other theoretical studies, and the loads calculated by the design codes.

(iv) Discussion of the results of the present theory and their experimental verification.

(v) Recommendations for future studies.

It may be noted that in the present investigation, the plates are assumed to be thin, as well as geometrically perfect. The foundation is assumed to be a linear (Winkler) type. No attempt is made to delineate the effects of residual stresses in welded steel sheets.

Chapter 2

Elastic Buckling of Infinitely Long Plates on Elastic Foundations

The analysis of buckling of infinitely long plates resting on elastic foundations in this thesis is based on the following assumptions:

(i) The plate is considered geometrically perfect. For analysis in this chapter, it is considered to be made of an isotropic elastic material. It is assumed to be thin with respect to length and width dimensions. Its self weight is considered negligible. It is loaded by uniformly compressive stress in the longitudinal direction only. The boundary conditions are assumed to allow the plate to remain in in-plane equilibrium under slowly increasing magnitude of this stress, until a critical value is reached, at which point the plate buckles with wavy out-of-plane displacements. Thus, the buckling considered is of the bifurcation type.

(ii) The foundation is considered to be linear elastic, i.e., a Winkler foundation, with reaction forces proportional to the transverse deflections.

(iii) The plate is assumed to be supported without any bonding with the foundation, and without any friction present. The foundation thus provides resistance to only its compression, and is therefore termed as a tensionless foundation.

2.1 Governing equations of equilibrium

Fig. 2-1 shows the coordinate system with respect to the plate geometry. The longitudinal edges are at $y = 0$ and $y = b$. The pre-buckling state of stress is that of uniform uniaxial compression, $\sigma_{xx} = -\sigma$ or, equivalently, $N_{xx} = -\sigma t = -N$.

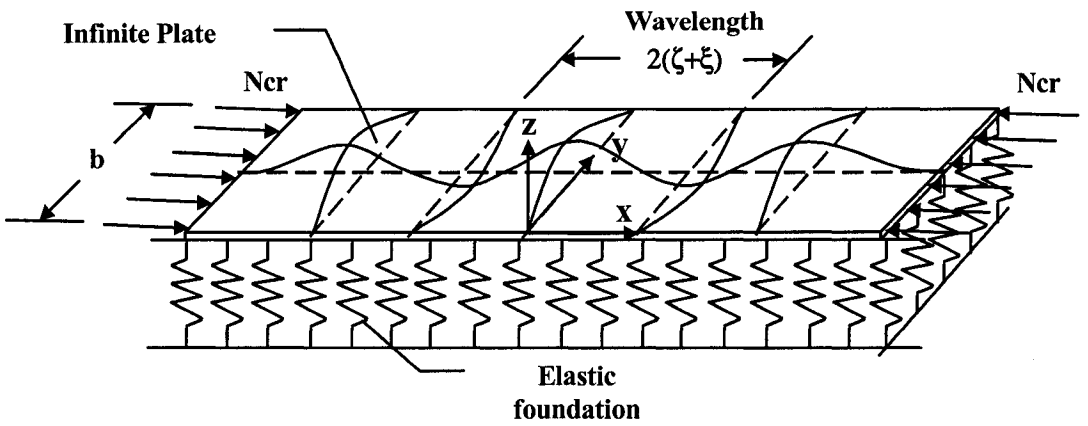

Fig. 2-1 Buckling mode of an infinitely long plate constrained unilaterally by an elastic foundation

For a bifurcation buckling analysis, only the out-of-plane displacement of the plate needs to be considered. This buckling displacement is denoted by $w(x, y)$, The three equations of equilibrium, two related to rotation in the x and y directions, and one related to translation in the z direction are (Fig. 2-2) as follows:

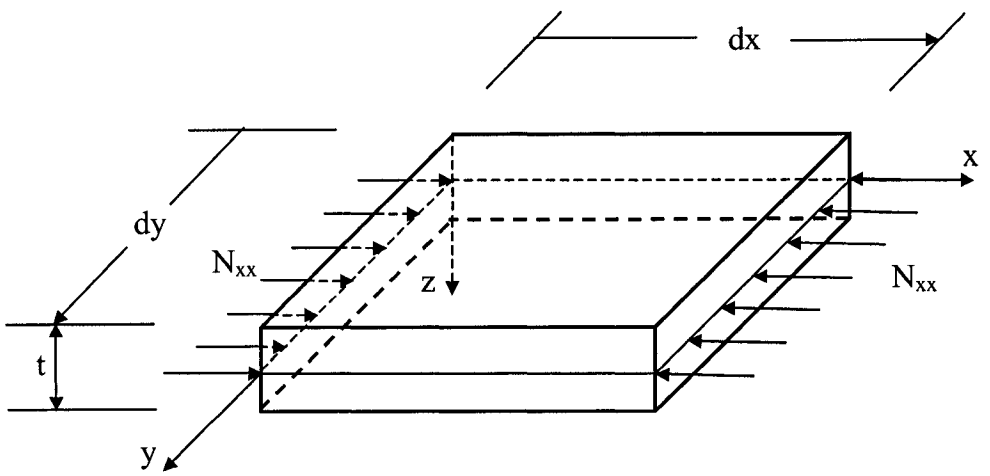

Fig. 2-2 Forces and moments acting on a plate coordinate element: (a) Axial force

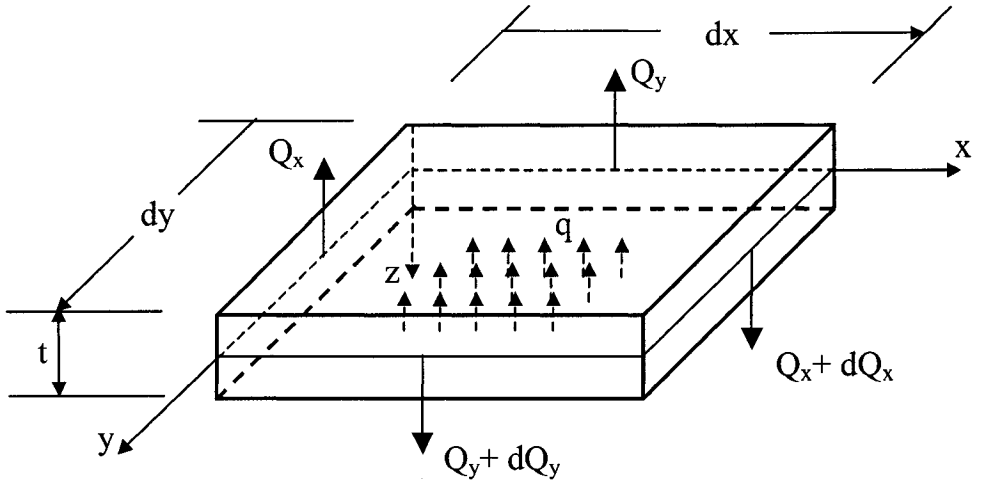

(b) Shear force

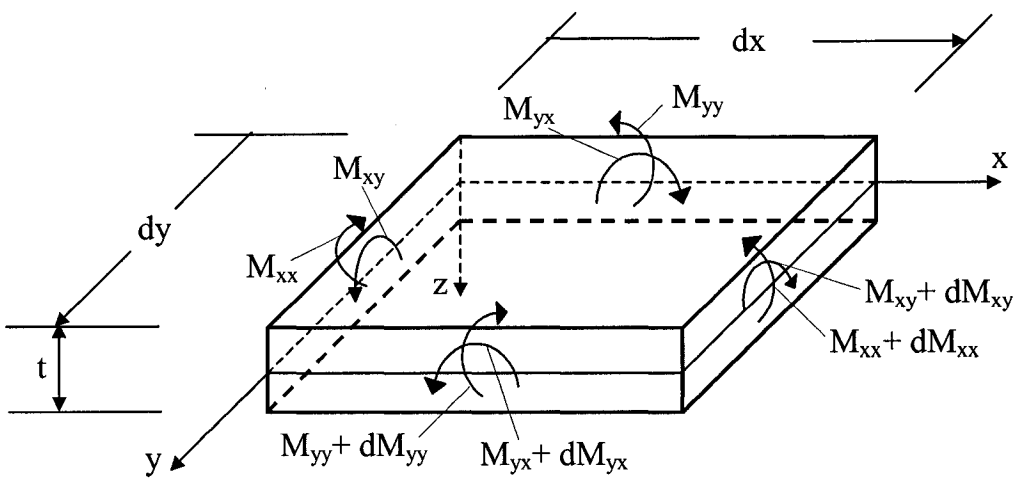

(c) Moment

Fig. 2-2 Forces and moments acting on a plate coordinate element

$$\frac{\partial M_{xx}}{\partial x} + \frac{\partial M_{xy}}{\partial y} - Q_x = 0$$

$$\frac{\partial M_{xy}}{\partial x} + \frac{\partial M_{yy}}{\partial y} - Q_y = 0$$

$$\frac{\partial Q_x}{\partial x} + \frac{\partial Q_y}{\partial y} - N_{\text{cr}}\frac{\partial^2 w}{\partial x^2} - kw = 0 \tag{2.1}$$

wherein M_{xx}, M_{yy}, $M_{xy} = M_{yx}$ are moment stress resultants per unit length, Q_x, Q_y are the shear stress resultants per unit length, and k is the foundation modulus equal to the reaction force per unit area and per unit deflection of the plate. The expressions for the three moment stress resultants relating to the stresses are:

$$M_{xx} = \int_{-\frac{t}{2}}^{\frac{t}{2}} z\,\sigma_{xx}\,dz,\; M_{yy} = \int_{-\frac{t}{2}}^{\frac{t}{2}} z\,\sigma_{yy}\,dz,\; M_{xy} = M_{yx} = \int_{-\frac{t}{2}}^{\frac{t}{2}} z\,\sigma_{xy}\,dz \tag{2.2}$$

The shear stress resultants Q_x and Q_y may be expressed as:

$$Q_x = \int_{-\frac{t}{2}}^{\frac{t}{2}} \sigma_{xz}\,dz,\; Q_y = \int_{-\frac{t}{2}}^{\frac{t}{2}} \sigma_{yz}\,dz \tag{2.3}$$

Now, the plate is considered thin, and thereby Kirchhoff assumptions are employed. These kinematic assumptions imply no strain in the thickness direction, and as well no transverse shear strains. In other words, irrespective of the material behaviour, it is assumed that $\epsilon_{zz} = \epsilon_{zx} = \epsilon_{zy} = 0$. These conditions are fulfilled by assuming that the fibers normal to the undeformed middle $(z = 0)$ surface undergo no length change and remain normal to the deformed middle surface, In effect the three coordinate displacement functions are taken as

$$u(x,y) = -z\frac{\partial w}{\partial x},\; v(x,y) = -z\frac{\partial w}{\partial y},\; w = w(x,y) \tag{2.4}$$

with corresponding non-zero strains as

$$\epsilon_{xx} = -z\frac{\partial^2 w}{\partial x^2},\; \epsilon_{yy} = -z\frac{\partial^2 w}{\partial x^2},\; \epsilon_{xy} = -z\frac{\partial^2 w}{\partial x \partial y} \tag{2.5}$$

Now, the stress assumptions are invoked, again irrespective of the particular material behaviour. It is assumed that $\sigma_{zz} = 0$, and the transverse shear stresses σ_{xz}, σ_{yz}, although non-zero, are not determinable from the stress-strain law. Their resultants Q_x, Q_y are however determinable from equations of equilibrium. The applicable stress-strain relations therefore involve only the in-plane stress and strain components. For linear elastic behaviour they are

$$\sigma_{xx} = \frac{E}{1-\nu^2}(\epsilon_{xx} + \nu\epsilon_{yy}\ ),\ \sigma_{yy} = \frac{E}{1-\nu^2}(\nu\epsilon_x\ + \epsilon_y),\ \sigma_{xy} = 2\,G\epsilon_{xy} \tag{2.6}$$

where E is Young's modulus and ν is Poisson's ratio. G is shear modulus, $G = \dfrac{E}{2(1+\nu)}$.

These expressions for stresses when substituted in the definitions of moment resultants lead to

$$M_{xx} = \int_{-\frac{t}{2}}^{\frac{t}{2}} z\,\sigma_{xx}\,dz = -D\,(\frac{\partial^2 w}{\partial x^2} + \nu\frac{\partial^2 w}{\partial y^2})$$

$$M_{yy} = \int_{-\frac{t}{2}}^{\frac{t}{2}} z\,\sigma_{yy}dz = -D\,(\nu\frac{\partial^2 w}{\partial x^2} + \frac{\partial^2 w}{\partial y^2})$$

$$M_{xy} = \int_{-\frac{t}{2}}^{\frac{t}{2}} z\,\sigma_{xy}dz = -D(1-\nu)\frac{\partial^2 w}{\partial x \partial y} \tag{2.7}$$

where $D = \dfrac{Et^3}{12(1-\nu^2)}$ is called the flexural rigidity of the plate. The equations of equilibrium now become

$$Q_x = -D\,(\frac{\partial^3 w}{\partial x^3} + \frac{\partial^3 w}{\partial x\ \partial y^2})$$

$$Q_y = -D\,(\frac{\partial^3 w}{\partial x^2 \partial y} + \frac{\partial^3 w}{\partial y^3})$$

$$D\,(\frac{\partial^4 w}{\partial x^4} + 2\frac{\partial^4 w}{\partial x^2\ \partial y^2} + \frac{\partial^4 w}{\partial y^4}) + N_{cr}\frac{\partial^2 w}{\partial x^2} + kw = 0 \tag{2.8}$$

The third equation in (2.8) is the governing equation of the problem. This equation poses an eigenvalue problem for determining N_{cr}, and has to be solved with stipulated boundary conditions on the edges.

The buckling of a long plate in the presence of a tensionless foundations will occur with two distinct regions of deformation, one with contact and the other without contact with the foundation. Since the plate is considered infinitely long in the x direction, there will be an infinite number of buckling waves in this direction. On the other hand, since the plate is of finite width in the y direction, it is reasonable to assume that the minimum buckling load would correspond to only a single buckle in this direction. The way the plate would lift up in some areas, and would compress the foundation in other areas, is shown in Fig. 2-1.

Let $w_1(x_1, y)$ and $w_2(x_2, y)$ represent the out-of-plane deflections in the contact $(k \neq 0)$ regions and no-contact $(k = 0)$ regions respectively. Then the applicable differential equations are

$$D(\frac{\partial^4 w_1}{\partial x_1^4} + 2\frac{\partial^4 w_1}{\partial x_1^2 \partial y^2} + \frac{\partial^4 w_1}{\partial y^4}) + N_{cr}\frac{\partial^2 w_1}{\partial x_1^2} + k w_1 = 0 \tag{2.9}$$

in the contact areas, and

$$D(\frac{\partial^4 w_2}{\partial x_2^4} + 2\frac{\partial^4 w_2}{\partial x_2^2 \partial y^2} + \frac{\partial^4 w_2}{\partial y^4}) + N_{cr}\frac{\partial^2 w_2}{\partial x_2^2} = 0 \tag{2.10}$$

in the no-contact areas.

In an effort to effect a separation of variables, solutions in the product form:

$$w_1(x_1, y) = \phi_1(x_1) * \psi(y) \tag{2.11}$$

$$w_2(x_2, y) = \phi_2(x_2) * \psi(y) \tag{2.12}$$

are sought where $\phi_1(x_1)$ and $\phi_2(x_2)$ are functions of x alone, and $\psi(y)$ is a function of y alone. x_1 is the x coordinate in the contact region, whereas x_2 is that in the no-contact region, as shown in Fig. 2-3. Thus, one obtains

$$D(\psi\frac{d^4\phi_1}{dx_1^4}+2\frac{d^2\phi_1}{dx_1^2}\frac{d^2\psi}{dy^2}+\phi_1\frac{d^4\psi}{dy^4})+N_{cr}\psi\frac{d^2\phi_1}{dx_1^2}+k\,\phi_1\psi=0 \tag{2.13}$$

in the contact areas, and

$$D(\psi\frac{d^4\phi_2}{dx_2^4}+2\frac{d^2\phi_2}{dx_2^2}\frac{d^2\psi}{dy^2}+\phi_2\frac{d^4\psi}{dy^4})+N_{cr}\psi\frac{d^2\phi_2}{dx_2^2}=0 \tag{2.14}$$

in the no-contact areas. From these equations it is apparent that a separation of variables is possible if

$\frac{d^2\psi}{dy^2}=-\mu^2\psi$, or equivalently, if

$$\psi=K_1\sin\mu y+K_2\cos\mu y \tag{2.15}$$

where K_1 and K_2 are arbitrary constants. For plates simply supported on sides $y=0$ and $y=b$, one must have $\mu=\frac{n\pi}{b}$ where n is an integer equal to the number of half waves in the y direction. It will be assumed on physical grounds that $n=1$ corresponds to the least bifurcation load, i.e., the critical load. In the further analysis it will be assumed that $\mu=\frac{\pi}{b}$ and, $\psi=\sin\mu y$.

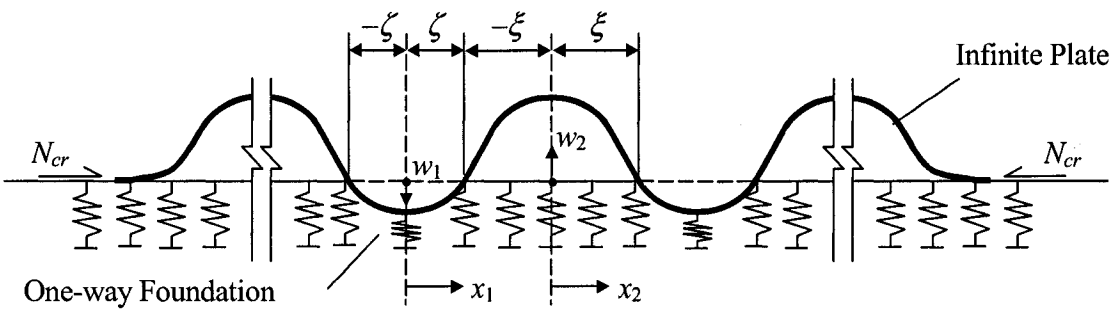

Fig. 2-3 Longitudinal section of buckling mode of an infinitely long plate resting on a one-way elastic foundation

2.2 Buckling deflections in contact and no-contact zones

2.2.1 Solution for buckling deflections in contact zones

From the above, the differential equation (2.13) valid for the contact region can be written as

$$\frac{d^4\phi_1}{dx_1^4} + \Gamma_1 \frac{d^2\phi_1}{dx_1^2} + \Gamma_2 \phi_1 = 0 \tag{2.16}$$

where

$$\Gamma_1 = \frac{N_{cr}}{D} - 2\mu^2, \Gamma_2 = \mu^4 + \frac{k}{D} \tag{2.17}$$

It is to be noted that while Γ_2 is always a positive number, Γ_1 is unrestricted. To find the solution of this ordinary differential equation with constant coefficients, let $\phi_1(x_1) = a_1 e^{mx_1}$ where a_1 is an arbitrary constant. Then, satisfaction of the differential equation requires that m be a root of

$$m^4 + \Gamma_1 m^2 + \Gamma_2 = 0 \tag{2.18}$$

Solving the quadratic equation, one obtains

$$m^2 = \frac{1}{2}(-\Gamma_1 \pm \sqrt{\Delta})$$

where

$$\Delta = \Gamma_1^2 - 4\Gamma_2 = \frac{N_{cr}}{D}(\frac{N_{cr}}{D} - 2\mu^2) - \frac{4k}{D} \tag{2.19}$$

Δ can be negative, positive, or zero. Hence all three possibilities must be considered.

Consider first the case $\Delta < 0$, or equivalently $4\Gamma_2 > \Gamma_1^2$, The four roots are the following complex conjugate pairs.

$$m_1 = c_1 + id_1,\, m_2 = c_1 - id_1,\, m_3 = -c_1 + id_1,\, ,\, m_4 = -c_1 - id_1; \tag{2.20}$$

where

$$c_1 = \frac{1}{2}\sqrt{2\sqrt{\Gamma_2} - \|\Gamma_1\|}\,,\; d_1 = \frac{1}{2}\sqrt{2\sqrt{\Gamma_2} + \|\Gamma_1\|} \tag{2.21}$$

The solution can therefore be written as

$$\begin{aligned}\phi_1(x_1) = {} & A_1'\cosh(c_1x_1)\cos(d_1x_1) + A_2'\cosh(c_1x_1)\sin(d_1x_1) + \\ & + A_3'\sinh(c_1x_1)\cos(d_1x_1) + A_4'\sinh(c_1x_1)\sin(d_1x_1)\end{aligned} \tag{2.22}$$

where constants A_1', A_2', A_3', and A_4' depend in general on the matching conditions with the solution for the contactless part. Now if the origin for this solution is taken at the centre of the buckle, then the solution must be symmetric about $x_1 = 0$. This symmetry condition requires $A_2' = A_3' = 0$. Hence the solution becomes

$$\phi_1(x_1) = A_1'\cosh(c_1x_1)\cos(d_1x_1) + A_4'\sinh(c_1x_1)\sin(d_1x_1) \tag{2.23}$$

From Fig. 2-3, it is apparent that at the ends, $x_1 = \pm\zeta$ of this buckle, $\phi_1(\pm\zeta) = 0$, which then requires

$$A_1' = -A_4'\tan(d_1\zeta)\tanh(c_1\zeta) \tag{2.24}$$

and finally the solution for this case ($\Delta < 0$) of roots is expressible as

$$\phi_1(x_1) = A_4'\,\{\sinh(c_1x_1)\sin(d_1x_1) - \tanh(c_1\zeta)\tan(d_1\zeta)\cosh(c_1x_1)\cos(d_1x_1)\} \tag{2.25}$$

Since $A_4'$is arbitrary, it is permissible to replace it as $A_4' = \dfrac{A}{c_1}$ and write

$$\phi_1(x_1) = \frac{A}{c_1}\{\sinh(c_1x_1)\sin(d_1x_1) - \tanh(c_1\zeta)\tan(d_1\zeta)\cosh(c_1x_1)\cos(d_1x_1)\} \tag{2.26}$$

The advantage of this change is that the solution in this form is valid for all values of c_1, real, zero, or purely imaginary. When $\Delta = 0$, or equivalently when $4\,\Gamma_2 = \Gamma_1^2$, it is found that $c_1 = 0$, and the above solution becomes the limit as $c_1 \to 0$,

$$\phi_1(x_1) = A\{x_1 \sin(d_1 x_1) - \zeta \tan(d_1\zeta)\cos(d_1 x_1)\} \tag{2.27}$$

Finally, if $\Delta > 0$, or equivalently if $4\,\Gamma_2 < \Gamma_1^2$, then $c_1 = i\,c_1'$ = purely imaginary, and the general solution becomes, with $c_1 = i\,c_1'$

$$\phi_1(x_1) = \frac{A}{i\,c_1'}\{\sinh(i\,c_1' x_1)\sin(d_1 x_1) - \tanh(i\,c_1'\zeta)\tan(d_1\zeta)\cosh(i\,c_1' x_1)\cos(d_1 x_1)\} \tag{2.28}$$

or, upon using the connection between hyperbolic and trigonometric functions,

$$\phi_1(x_1) = \frac{A}{c_1'}\{\sin(c_1' x_1)\sin(d_1 x_1) - \tan(c_1'\zeta)\tan(d_1\zeta)\cos(c_1' x_1)\cos(d_1 x_1)\} \tag{2.29}$$

which is of the same form, as when $\Delta > 0$ is treated separately as a special case.

2.2.2 Solution for buckling deflections in no-contact zones

When there is no contact with the foundation, the modulus $k = 0$, and the separated equation reads

$$\frac{d^4\phi_2}{dx_2^4} + \Gamma_1' \frac{d^2\phi_2}{dx_2^2} + \Gamma_2'\,\phi_2 = 0 \tag{2.30}$$

in which

$$\Gamma_1' = \frac{N_{cr}}{D} - 2\,\mu^2\ (= \Gamma_1, \text{ same as before}), \text{ and } \Gamma_2' = \mu^4 \tag{2.31}$$

$$\Gamma_1'^2 - 4\Gamma_2' = \frac{N_{cr}}{D} - 4\,\mu^2 \tag{2.32}$$

Analogous to the analysis for the contact cases, one must now find the applicable solutions. Assuming $\phi_2(x_2) = a_2 e^{n x_2}$ where a_2 is some constant, it is found that for it to be a solution of the differential equation, n must be a root of

$$n^4 + \Gamma_1' n^2 + \Gamma_2' = 0 \tag{2.33}$$

Solving the quadratic equation, one obtains

$$n^2 = \frac{1}{2}(-\Gamma_1' \pm \sqrt{\Delta'}) \tag{2.34}$$

where

$$\Delta' = \Gamma_1'^2 - 4\Gamma_2' = (\frac{N_{cr}}{D} - 2\mu^2) \tag{2.35}$$

Again three cases of roots might arise. However, by using the device introduced earlier, all three cases can be considered by one formula. Let $\Delta' < 0$, or equivalently $4\Gamma_2' > \Gamma_1'^2$, The four roots are the following complex conjugate pairs:

$$n_1 = c_2 + id_2, n_2 = c_2 - id_2, n_3 = -c_2 + id_2, , n_4 = -c_2 - id_2; \tag{2.36}$$

where

$$c_2 = \frac{1}{2}\sqrt{2\sqrt{\Gamma_2'} - \|\Gamma_1'\|}\,, d_2 = \frac{1}{2}\sqrt{2\sqrt{\Gamma_2'} + \|\Gamma_1'\|} \tag{2.37}$$

The solution can therefore be written as

$$\begin{aligned}\phi_2(x_2) = {} & B_1'\cosh(c_2x_2)\cos(d_2x_2) + B_2'\cosh(c_2x_2)\sin(d_2x_2) \\ & + B_3'\sinh(c_2x_2)\cos(d_2x_2) + B_4'\sinh(c_2x_2)\sin(d_2x_2)\end{aligned} \tag{2.38}$$

where constants B_1', B_2', B_3', and B_4' depend in general on the matching conditions with the solution for the contact part. Now if the origin for this solution is taken at the centre of the buckle then the solution must be symmetric about $x_2 = 0$. This symmetry condition requires $B_2' = B_3' = 0$. Hence the solution becomes

$$\phi_2(x_2) = B_1'\cosh(c_2x_2)\cos(d_2x_2) + B_4'\sinh(c_2x_2)\sin(d_2x_2) \tag{2.39}$$

The length of a typical contactless buckle is taken as 2ξ, with origin at the centre of the buckle. Then the symmetric condition, $\phi_2(-x_2) = \phi_2(x_2)$, plus the fact that the deflection is zero at the ends of the buckle, $\phi_2(\pm\xi) = 0$, Fig. 2-3, it is found that the solution may be written as

$$\phi_2(x_2) = \frac{B}{c_2}\{\sinh(c_2x_2)\sin(d_2x_2) - \tanh(c_2\xi)\tan(d_2\xi)\cosh(c_2x_2)\cos(d_2x_2)\} \qquad (2.40)$$

where B is a constant. As before this form of the solution is applicable to all three cases of $\Delta' < 0$, $\Delta' = 0$, and $\Delta' > 0$. Similar to the case of $\Delta' < 0$, setting $c_2 = i\,c_2'$ the formula of the deflection in contactless zones for $\Delta' > 0$ follows

$$\phi_2(x_2) = \frac{B}{c_2'}\{\sin(c_2'x_2)\sin(d_2x_2) - \tan(c_2'\xi)\tan(d_2\xi)\cos(c_2'x_2)\cos(d_2x_2)\} \qquad (2.41)$$

2.3 Matching conditions between contact and no-contact regions

In the previous section, separate solutions were obtained for the contact and no-contact regions of the buckled plate. Since they belong to the same plate, they must be compatible along the common edges between the two parts. At these edges the two solutions must have the same deflection, same slope, same bending moment, and same shear. As shown in Fig. 2-3, the common edges occur at $x_1 = \zeta$ for the contact part, ant at $x_2 = -\xi$ for the no-contact part. The equality of deflections, has already been accounted for by requiring them to be zero at the common edges. The remaining matching conditions are

$$\left.\frac{dw_1}{dx_1}\right|_{x_1=\zeta} = \left.\frac{dw_2}{dx_2}\right|_{x_2=-\xi} \qquad (2.42)$$

$$\left.M_{xx}\right|_{x_1=\zeta} = \left.M_{xx}\right|_{x_2=-\xi} \qquad (2.43)$$

$$\left.Q_x\right|_{x_1=\zeta} = \left.Q_x\right|_{x_2=-\xi} \qquad (2.44)$$

The first equation, by virtue of the product solutions (2.11) and (2.12) leads to the equality of the first derivatives, as

$$\left.\frac{d\phi(x_1)}{dx_1}\right|_{x_1=\zeta} = \left.\frac{d\phi(x_2)}{dx_2}\right|_{x_2=-\xi} \qquad (2.45)$$

For the second condition, recall the expression (2.7) for the bending moment M_{xx} in terms of the derivatives of deflection. For example,

$$M_{xx}\Big|_{x_1=\zeta} = -D\left(\frac{\partial^2 w_1}{\partial x_1^2} + \nu\frac{\partial^2 w_1}{\partial y^2}\right)\Big|_{x_1=\zeta} \tag{2.46}$$

Now, since $w_1(x_1, y) = \phi_1(x_1)\psi(y)$, and $\phi_1(\zeta) = 0$, the above equation becomes

$$M_{xx}\Big|_{x_1=\zeta} = -D\frac{d^2\phi_1(x_1)}{dx_1^2}\psi(y)\Big|_{x_1=\zeta} \tag{2.47}$$

In a similar fashion, for the no-contact zone it follows that

$$M_{xx}\Big|_{x_2=-\xi} = -D\frac{d^2\phi_2(x_2)}{dx_2^2}\psi(y)\Big|_{x_2=-\xi} \tag{2.48}$$

Hence, regardless of $\psi(y)$, the equality of the bending moments at the common edges requires equality of the second derivatives of the two solutions:

$$\frac{d^2\phi(x_1)}{dx_1^2}\Big|_{x_1=\zeta} = \frac{d^2\phi_2(x_2)}{dx_2^2}\Big|_{x_2=-\xi} \tag{2.49}$$

The expression for the shear force Q_x at the common edge as part of the contact zone is,

$$Q_x\Big|_{x_1=\zeta} = -D\frac{\partial}{\partial x_1}\left(\frac{\partial^2 w_1}{\partial x_1^2} + \nu\frac{\partial^2 w_1}{\partial y^2}\right)\Big|_{x_1=\zeta} \tag{2.50}$$

which, in view of the product solution (2.11) and (2.12), reduces to

$$Q_x\Big|_{x_1=\zeta} = -D\left(\frac{d^3\phi_1(x_1)}{dx_1^3}\psi(y) + \nu\frac{d^2\psi(y)}{dy^2}\frac{d\phi_1(x_1)}{dx_1}\right)\Big|_{x_1=\zeta} \tag{2.51}$$

Analogously, the expression for the no-contact zone reduces to

$$Q_x\Big|_{x_2=-\xi} = -D\left(\frac{d^3\phi_2(x_2)}{dx_2^3}\psi(y) + \nu\frac{d^2\psi(y)}{dy^2}\frac{d\phi_2(x_2)}{dx_2}\right)\Big|_{x_2=-\xi} \tag{2.52}$$

Hence, in view of the matching of the first derivatives of the two solutions, the equality of the shears requires equality of the third derivatives, i.e.,

$$\frac{d^3\phi_1(x_1)}{dx_1^3}\Big|_{x_1=\zeta} = \frac{d^3\phi_2(x_2)}{dx_2^3}\Big|_{x_2=-\xi} \tag{2.53}$$

To summarize, the four matching conditions reduce to equality of the three successive derivatives together with the functions being zero at the common edges. These conditions have been derived on the basis of the product solution, but without regard to the specific nature of the function $\psi(y)$. This observation is important for the product solutions to be obtained by the virtual work method.

These conditions are used to determine buckling load and wavelength equations in the next section.

2.4 Equations for buckling loads and wavelengths by the equilibrium method

Let the first derivatives at the common edges of the two regions be expressed as

$$Aa_{11} = Aa_{11}(\zeta) = \frac{d\phi_1(x_1)}{dx_1}\Big|_{x_1=\zeta} \text{ and } Ba_{12}(\xi) = \frac{d\phi_2(x_2)}{dx_2}\Big|_{x_2=-\xi} \tag{2.54}$$

which, as indicated, are evaluated after performing the indicated differentiation, and where it may be noted that while a_{11} is a function of ζ, a_{12} is that of ξ. The equality of the first derivatives requires that

$$a_{11}A - a_{12}B = 0 \tag{2.55}$$

Similarly, the equality of the second and third derivatives may be expressed as

$$\begin{aligned} a_{21}A - a_{22}B &= 0 \\ a_{31}A - a_{32}B &= 0 \end{aligned} \tag{2.56}$$

where

$$Aa_{21} = Aa_{21}(\zeta) = \frac{d^2\phi_1(x_1)}{dx_1^2}\Big|_{x_1=\zeta} \text{ and } Ba_{22}(\xi) = \frac{d^2\phi_2(x_2)}{dx_2^2}\Big|_{x_2=-\xi} \tag{2.57}$$

$$Aa_{31} = Aa_{31}(\zeta) = \frac{d^3\phi_1(x_1)}{dx_1^3}\Big|_{x_1=\zeta} \text{ and } Ba_{32}(\xi) = \frac{d^3\phi_2(x_2)}{dx_2^3}\Big|_{x_2=-\xi} \tag{2.58}$$

are evaluated as indicated. A *Mathematica* [20] program can be written to obtain the coefficients a_{11}, a_{12} etc.

Apparently, there are thus three equations with two unknowns A and B. However, the fact is that the length of buckling regions 2ζ and 2ξ and the buckling load also are unknowns of the problem. The constants A and B are eliminated between two pairs of the above equations as follows. Thus, elimination of A and B from the first and second, and from first and third, gives the following two equations:

$$a_{11}a_{22} - a_{12}a_{21} = 0 \tag{2.59}$$

$$a_{11}a_{32} - a_{12}a_{31} = 0 \tag{2.60}$$

The third relation obtained from second and third equations (2.56), $a_{21}a_{32} - a_{22}a_{31} = 0$, is a linear combination of the previous two, and is therefore an identity. This relation is not used in the following, but it might be used as a check on the accuracy of the numerical results. The two equations may be called the buckling equations, are expressible as

$$\begin{aligned}\text{Eq1} = {} & d_2\text{sech}(c_2\xi)\text{sec}(d_2\xi)\{\cos(2d_2\xi) + \cosh(2c_2\xi)\}* \\ & \{\text{sech}(\text{c}_1\zeta)\sin(d_1\zeta)+\frac{d_1}{c_1}\sinh(c_1\zeta)\text{sec}(d_1\zeta)\} - d_1\text{sech}(\text{c}_1\zeta)\text{sec}(d_1\zeta)\{\cos(2d_1\zeta) + \\ & \cosh(2c_1\zeta)\}*\{\text{sech}(\text{c}_2\xi)\sin(d_2\xi)+\frac{d_2}{c_2}\sinh(c_2\xi)\text{sec}(d_2\xi)\} = 0\end{aligned} \tag{2.61}$$

$$\begin{aligned}\text{Eq2} = {} & -\{(\text{c}_1^2 - 3\,d_1^2)\text{sech}(\text{c}_1\zeta)\sin(d_1\zeta)+\frac{d_1}{c_1}(3\text{c}_1^2 - d_1^2)\sinh(c_1\zeta)\text{sec}(d_1\zeta)\}\{\text{sech}(\text{c}_2\xi)* \\ & \sin(d_2\xi) + \frac{d_2}{c_2}\sinh(\text{c}_2\xi)\text{sec}(d_2\xi)\} + \{\text{sech}(\text{c}_1\zeta)\sin(d_1\zeta)+\frac{d_1}{c_1}\sinh(c_1\zeta)\text{sec}(d_1\zeta)\}* \\ & \{(\text{c}_2^2 - 3\,d_2^2)\,\text{sech}(\text{c}_2\xi)\sin(d_2\xi) + \frac{d_2}{c_2}(3\text{c}_2^2 - d_2^2)\sinh(c_2\xi)\text{sec}(d_2\xi)\} = 0\end{aligned} \tag{2.62}$$

These equations can be simplified as the following two equations

$$\text{Eq1} = \frac{1}{c_1 d_1}\frac{\{c_1\sin(2d_1\zeta)+d_1\sinh(2c_1\zeta)\}}{\{\cos(2d_1\zeta)+\cosh(2c_1\zeta)\}} - \frac{1}{c_2 d_2}\{\frac{c_2\sin(2d_2\xi)+d_2\sinh(2c_2\xi)}{\cos(2d_2\xi)+\cosh(2c_2\xi)}\} = 0 \tag{2.63}$$

$$\text{Eq2} = \frac{1}{c_1 d_1}\frac{\{c_1\sin(2d_1\zeta)+d_1\sinh(2c_1\zeta)\}}{\{(c_1^2-3\,d_1^2)\sin(2d_1\zeta)+\frac{d_1}{c_1}(3c_1^2-d_1^2)\sinh(2c_1\zeta)\}} + $$
$$- \frac{1}{c_2 d_2}\frac{\{c_2\sin(2d_2\xi)+d_2\sinh(2c_2\xi)\}}{\{(c_2^2-3\,d_2^2)\sin(2d_2\xi)+\frac{d_2}{c_2}(3c_2^2-d_2^2)\sinh(2c_2\xi)\}} = 0 \tag{2.64}$$

These latter equations are more convenient for the trial and error procedure of solving them. For a plate of given dimensions, b and t, material properties, E and ν, and a given foundation modulus k, the way these equations are used to calculate the minimum N_{cr} and the corresponding buckle lengths 2ζ and 2ξ is explained later in Section 2.6.

2.5 Equations for buckling loads and wavelengths by the method of virtual work

The above analysis is exact in the sense that no mathematical approximations were made to arrive at the solution. This was possible because the boundary conditions of simply supports at $y = 0,\ b$ allowed separation of variables. For other boundary conditions at these edges, say fixed edges, one may resort to the method of virtual work or energy methods to find approximate analytical solutions. Using the energy method, the buckling loads for infinitely long orthotropic elastic plates resting on one-way elastic foundations were derived in Ref. [17].

Here, the more general method of virtual work is adopted. For a buckled plate the virtual work expression, assuming validity of the Kirchhoff kinematic hypothesis, is

$$\delta W = -\int_A (M_{xx}\frac{\partial^2 \delta\, w}{\partial x^2} + M_{yy}\frac{\partial^2 \delta\, w}{\partial y^2} + 2M_{xy}\frac{\partial^2 \delta\, w}{\partial x \partial y})dA$$
$$-\int_A N_{cr}\frac{\partial\, w}{\partial x}\frac{\partial\, \delta w}{\partial x}dA + \int_A F\,\delta w\, dA \tag{2.65}$$

where w and δw are respectively the actual and virtual displacements of the plate, N_{cr} is the buckling load per unit length of the side of the plate, A here denotes the area of the plate, and F is the foundation reaction force per unit area of the plate.

Let the general relations between stress and strain increments arising due to bifurcation buckling be written as

$$\sigma_{xx} = \overline{B}\epsilon_{xx} + \overline{C}\epsilon_{yy},\ \sigma_{yy} = \overline{C}\epsilon_{xx} + \overline{D}\epsilon_{yy},\ \sigma_{xy} = 2\overline{F}\epsilon_{xy} \tag{2.66}$$

where $\overline{B}$, $\overline{C}$, $\overline{D}$, $\overline{F}$ are appropriate moduli at the bifurcation state. These moduli are assumed constant throughout the plate body. Now, according to Kirchhoff hypothesis, the strains are related to the displacement derivatives as

$$\epsilon_{xx} = -z\frac{\partial^2 w}{\partial x^2},\ \epsilon_{yy} = -z\frac{\partial^2 w}{\partial y^2},\ \epsilon_{xy} = -z\frac{\partial^2 w}{\partial x \partial y} \tag{2.67}$$

which when substituted in the constitutive relations (2.7), give the moment resultants, upon invoking their definitions, as

$$M_{xx} = -\frac{t^3}{12}(\overline{B}\frac{\partial^2 w}{\partial x^2} + \overline{C}\frac{\partial^2 w}{\partial y^2}),\ M_{yy} = -\frac{t^3}{12}(\overline{C}\frac{\partial^2 w}{\partial x^2} + \overline{D}\frac{\partial^2 w}{\partial y^2}),\ M_{xy} = -\frac{2t^3}{12}\overline{F}\frac{\partial^2 w}{\partial x \partial y} \tag{2.68}$$

The virtual work expression can therefore be written as

$$\delta W = \frac{t^3}{12}\int_A \{(\overline{B}\frac{\partial^2 w}{\partial x^2} + \overline{C}\frac{\partial^2 w}{\partial y^2})\frac{\partial^2 \delta w}{\partial x^2} + (\overline{C}\frac{\partial^2 w}{\partial x^2} + \overline{D}\frac{\partial^2 w}{\partial y^2})\frac{\partial^2 \delta w}{\partial y^2} + 4\overline{F}\frac{\partial^2 w}{\partial x \partial y}\frac{\partial^2 \delta w}{\partial x \partial y}\}dA$$

$$-\int_A N_{cr}\frac{\partial w}{\partial x}\frac{\partial \delta w}{\partial x}dA + \int_A k\, w\, \delta w\, dA \tag{2.69}$$

where $F = k\,w$ has been substituted, k being the foundation modulus, which in the present case of tensionless foundation is allowed to be zero in the no-contact zones. The assumption is now made that the deflection is the product of two functions,

$$w(x, y) = \phi(x)\psi(y) \tag{2.70}$$

where $\psi(y)$ is a suitably chosen known function of y which satisfies the desired boundary conditions at $y = 0,\ b$ edges. Then $\psi(y)$ is not subject to any variation, and therefore

$$\delta w(x,y) = \delta\phi(x)\,\psi(y),$$

$$\frac{\partial \delta w}{\partial x} = \frac{d\delta\phi}{dx}\psi,\ \frac{\partial \delta w}{\partial y} = \delta\phi\frac{d\psi}{dy}$$

$$\frac{\partial^2 \delta w}{\partial x^2} = \frac{d^2\delta\phi}{dx^2}\psi,\ \frac{\partial^2 \delta w}{\partial y^2} = \delta\phi\frac{d^2\psi}{dy^2},\ \frac{\partial^2 \delta w}{\partial x \partial y} = \frac{d\delta\phi}{dx}\frac{d\psi}{dy} \tag{2.71}$$

With this assumption incorporated, one obtains

$$\delta W = \frac{t^3}{12}\int_A \{(\bar{B}\frac{d^2\phi}{dx^2}\psi^2 + \bar{C}\psi\frac{d^2\psi}{dy^2})\frac{d^2\delta\phi}{dx^2} + (\bar{C}\psi\frac{d^2\psi}{dy^2}\frac{d^2\phi}{dx^2} + \bar{D}(\frac{d^2\psi}{dy^2})^2\phi)\delta\phi + 4\bar{F}(\frac{d\psi}{dy})^2\frac{d\phi}{dx}\frac{d\delta\phi}{dx}\}dA$$

$$-\int_A N_{cr}\psi^2\frac{d\,\phi}{dx}\frac{d\,\delta\phi}{dx}dA + \int_A k\psi^2\,\delta\phi\,dA \tag{2.72}$$

Introducing the symbols

$$\bar{\psi}_1 = \int_0^b \psi^2 dy,\ \bar{\psi}_2 = \int_0^b \psi\frac{d^2\psi}{dy^2}dy,\ \bar{\psi}_3 = \int_0^b (\frac{d^2\psi}{dy^2})^2 dy,\ \bar{\psi}_4 = \int_0^b (\frac{d\,\psi}{dy})^2 dy \tag{2.73}$$

the virtual work expression can be written as

$$\delta W = \frac{t^3}{12}\int_x (\bar{B}\bar{\psi}_1\frac{d^2\phi}{dx^2} + \bar{C}\bar{\psi}_2\phi)\frac{d^2\delta\phi}{dx^2} + (\bar{C}\bar{\psi}_2\frac{d^2\phi}{dx^2} + \bar{D}\,\bar{\psi}_3\phi)\delta\phi + 4\bar{F}\,\bar{\psi}_4\frac{d\phi}{dx}\frac{d\delta\phi}{dx}\}dx$$

$$-\int_x N_{cr}\bar{\psi}_1\frac{d\,\phi}{dx}\frac{d\,\delta\phi}{dx}dx + \int_x k\,\bar{\psi}_1\phi\,\delta\phi\,dx \tag{2.74}$$

The integration is with respect to x, the longitudinal coordinate. Since the end points are at infinity, one is not interested in the boundary conditions, but only the differential equation. The latter is obtained as coefficient of $\delta\phi$, when integration by parts has reduced $\frac{d^2\delta\phi}{dx^2}$ and $\frac{d\delta\phi}{dx}$ to $\delta\phi$. The differential equation thus obtained is

$$\overline{B}\overline{\psi}_1\frac{d^4\phi}{dx^4} + (2\overline{C}\overline{\psi}_2 - 4\overline{F}\,\overline{\psi}_4 + N_{cr}\overline{\psi}_1)\frac{d^2\phi}{dx^2} + (\overline{D}\,\overline{\psi}_3 + k\,\overline{\psi}_1)\phi = 0 \tag{2.75}$$

Dividing throughout by $\overline{B}\overline{\psi}_1$ the above equation can be written in the form

$$\frac{d^4\phi}{dx^4} + \overline{\Gamma}_1\frac{d^2\phi}{dx^2} + \overline{\Gamma}_2\,\phi = 0 \tag{2.76}$$

where

$$\overline{\Gamma}_1 = \frac{1}{\overline{B}}(2\overline{C}\frac{\overline{\psi}_2}{\overline{\psi}_1} - 4\overline{F}\,\frac{\overline{\psi}_4}{\overline{\psi}_1} + N_{cr}),\ \overline{\Gamma}_2 = \frac{1}{\overline{B}}(\overline{D}\frac{\overline{\psi}_3}{\overline{\psi}_1} + k\,) \tag{2.77}$$

This equation is exactly of the same form as the equations (2.16) in the contact zones when $k \neq 0$ and (2.33) in no-contact zones when $k = 0$, which has been obtained in the case of simply supported plates by the equilibrium method, allowing separation of variables. For the no-contact zone, $k = 0$, and the coefficients for the differential equation for $\phi_2(x_2)$are

$$\overline{\Gamma}_1' = \frac{1}{\overline{B}}(2\overline{C}\frac{\overline{\psi}_2}{\overline{\psi}_1} - 4\overline{F}\,\frac{\overline{\psi}_4}{\overline{\psi}_1} + N_{cr}),\overline{\Gamma}_2' = \frac{\overline{D}}{\overline{B}}\frac{\overline{\psi}_3}{\overline{\psi}_1} \tag{2.78}$$

For linear elastic isotropic materials

$$\overline{B} = \overline{D} = \frac{Et^3}{12(1-\nu^{2)}} = D,\ \overline{C} = \nu\overline{B},\ 2\overline{F} = \overline{D} - \overline{C} \tag{2.79}$$

The coefficients become

$$\overline{\Gamma}_1 = 2\nu\frac{\psi_2}{\overline{\psi}_1} - 2(1-\nu)\,\frac{\overline{\psi}_4}{\overline{\psi}_1} + \frac{N_{cr}}{\overline{B}},\ \overline{\Gamma}_2 = (\,\frac{\overline{\psi}_3}{\overline{\psi}_1} + \frac{k}{D}\,),\ \overline{\Gamma}_2' = \frac{\overline{\psi}_3}{\overline{\psi}_1} \tag{2.80}$$

For a simply supported plate $\psi(y) = \sin\frac{\pi y}{b} = \sin\mu y$, where $\mu = \frac{\pi}{b}$, one finds

$$\overline{\psi}_1 = \frac{b}{2},\ \overline{\psi}_2 = -\frac{\pi^2}{2b} = ,\ \overline{\psi}_3 = \frac{\pi^4}{2b^3},\ \overline{\psi}_4 = \frac{\pi^2}{2b} \tag{2.81}$$

$$\overline{\Gamma}_1 = \frac{N_{cr}}{D} - \frac{2\pi}{b^2},\ \overline{\Gamma}_2 = (\frac{\pi^4}{b^4} + \frac{k}{D}),\ \overline{\Gamma}_2' = \frac{\pi^4}{b^4} \tag{2.82}$$

Hence, the coefficients in the differential equation become

$$\overline{\Gamma}_1 = (\frac{N_{cr}}{D} - 2\mu^2),\ \overline{\Gamma}_2 = (\mu^4 + \frac{k}{D}),\ \overline{\Gamma}_2' = \mu^4 \tag{2.83}$$

which then leads to the same differential equations as those obtained by the exact equilibrium method:

$$(\frac{d^4\phi_1}{dx_1^4} - 2\mu^2\frac{d^2\phi_1}{dx_1^2} + \mu^4\phi_1) + \frac{N_{cr}}{D}\frac{d^2\phi_1}{dx_1^2} + \frac{k}{D}\phi_1 = 0 \tag{2.84}$$

in contact regions, and

$$(\frac{d^4\phi_2}{dx_2^4} - 2\mu^2\frac{d^2\phi_2}{dx_2^2} + \mu^4\phi_2) + \frac{N_{cr}}{D}\frac{d^2\phi_2}{dx_2^2} = 0 \tag{2.85}$$

in contactless regions for the infinite isotropic plates, simply supported on unloaded edges.

2.6 Solutions of buckling loads and wavelengths for simply supported plates

The two buckling equations, Eqs. (2.63) and (2.64), obtained by the equilibrium method for the simply supported plate, are now solved to determine the minimum stress which would cause buckling. These equations are, however, nonlinear. In each of the two equations there are three variables, namely the buckling load N_{cr}, the contact area buckle length 2ζ, and the no-contact buckle length 2ξ. One cannot find a solution for three unknown variables from two equations. It is necessary to have a third condition. This condition is supplied by the fact that the buckling load N_{cr} must be a minimum. In the procedure adopted here, one assumes a value of 2ζ, the contact buckle length, and then finds the other two unknowns from the two buckling equations. This is done with different values of 2ζ (employing a trial and error procedure) until that value for which the buckling load N_{cr} has the lowest value. The corresponding variable 2ξ, the buckle length of the no-contact zones, is also then obtained. The *Mathematica* program for

doing these calculations can be constructed without much difficulty. The interested reader may also obtain the author's program by contacting him via the department address.

To incorporate with previous works, particularly Reference [17], the following non-dimensional quantities are introduced:

$$\lambda = \frac{N_{cr} b^2}{\pi^2 D}, \alpha = \frac{k b^4}{\pi^4 D} \tag{2.86}$$

Thus, N_{cr} is replaced by λ, and k is replaced by α. It may be recalled that the buckling load for an infinitely long simply supported plate, without a foundation, $N_{cr} = \frac{4\,\pi^2\,D}{b^2}$ corresponds to $\lambda = 4$. Therefore, naturally with a foundation present, $\lambda > 4$.

As mentioned previously, a *Mathematica* program was written to solve the buckling equations. A set of numerical results comprising of λ, ζ and ξ values were obtained for the simply supported plate. Table 2.1 lists these values for the tensionless foundation modulus k varying from 0 to ∞.

Table 2.1 λ, ζ and ξ for elastic infinitely long simply supported plates resting on different tensionless foundations

	$\alpha = 0$	$\alpha = 1.0$	$\alpha = 1000$	$\alpha = 1.0 \times 10^5$	$\alpha = \infty$
λ	4.0	4.332	5.316	5.333	5.333
ζ/b	0.5	0.414	0.075	0.024	0
ξ/b	0.5	0.535	0.759	0.832	0.866

Figure 2-4 provides a graph of λ versus α. Also shown on this graph are the results for the clamped plate, to be discussed later. The graph shows that as the foundation modulus increases the buckling load also increases. On the other hand, as shown in Fig. 2-5, the wavelength of the contact buckles decreases as the modulus increases, Inversely, the wavelength of no-contact regions increases. When α reaches a large value, (the foundation is then practically rigid), the bucking load coefficient λ reaches its maximum value of 5.333, the contact wavelength to width ratio ζ/b approximates 0, and the no-contact wavelength to width ξ/b reaches its highest value 0.866. The case $\zeta/b = 0$

means that the plate has only line contact and buckles unilaterally, i.e., only away from the foundation, Fig. 2-6.

The maximum value of $\lambda = 5.333$, means that the maximum increase in the buckling load due to a foundation is 33% over that when there is no foundation.

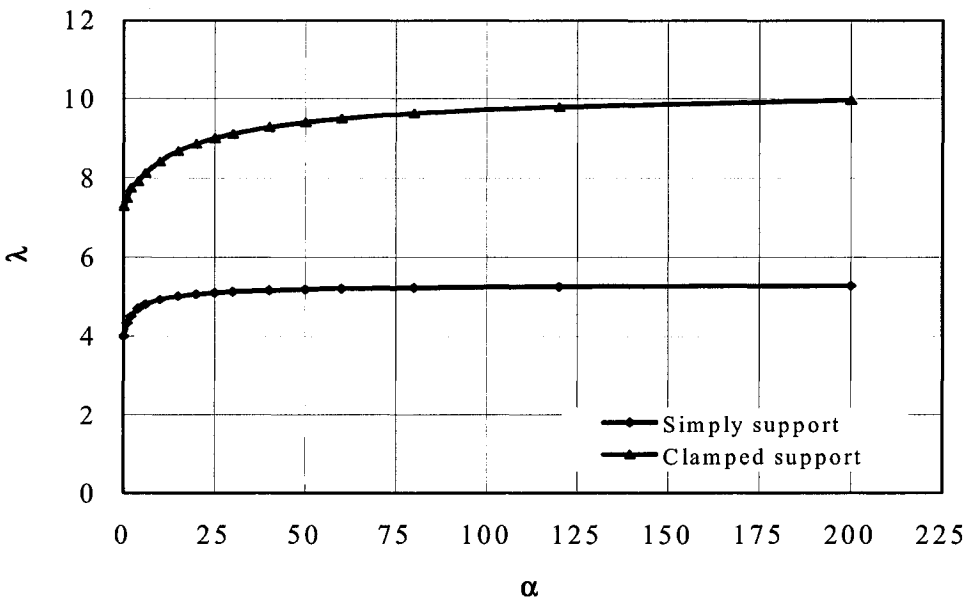

Fig. 2-4 Buckling load coefficient (λ) - foundation stiffness parameter (α) curves with different boundary conditions

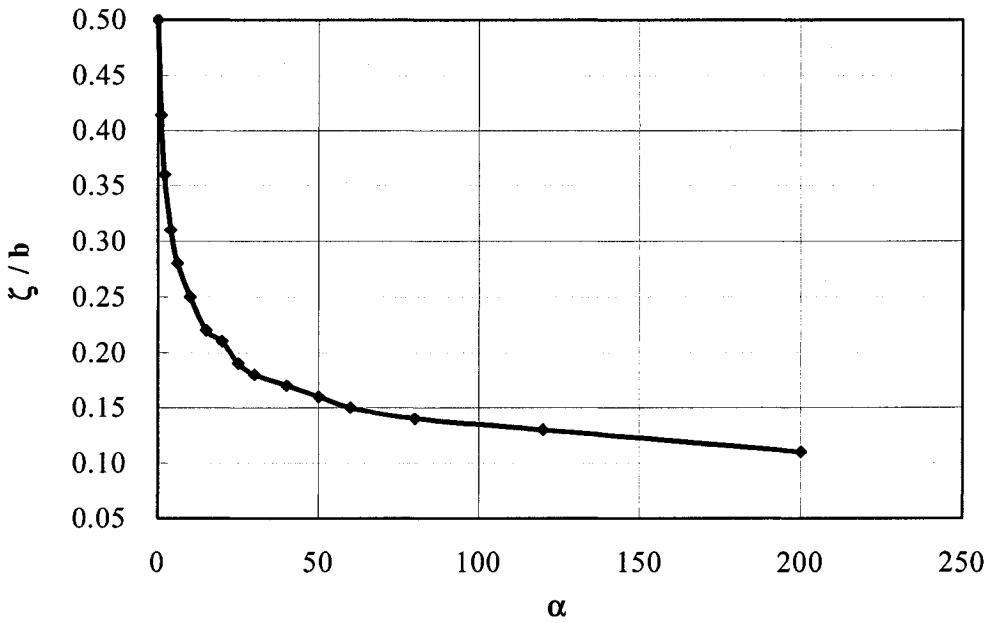

Fig. 2-5 Wavelength to width ratio - foundation stiffness parameter curves with simply supported unloaded edges

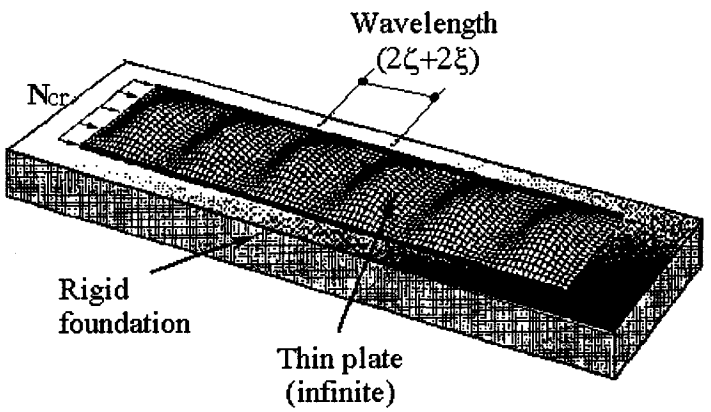

Fig. 2-6 Elastic buckling mode of an infinite plate resting on a rigid foundation [6]

2.7 Solutions of buckling loads and wavelengths under clamped edges

Following Ref. [17], it is assumed that for an infinitely long plate in x direction and clamped at the edges $y = 0, b$, a suitable solution is $w(x, y) = \phi(x)\sin^2(\frac{\pi y}{b})$ to represent the deflection of the plate. This choice of $\psi(y) = \sin^2(\frac{\pi y}{b})$ satisfies the conditions of deflections and slopes being zero at the longitudinal edges, i.e.,

$$w(x,0) = w(x,b) = \frac{\partial w(x,y)}{\partial y}|_{y=0} = \frac{\partial w(x,y)}{\partial y}|_{y=b} = 0 \tag{2.87}$$

$$\text{since } \psi(0) = \psi(b) = \frac{d\psi(y)}{dy}|_{y=0} = \frac{d\psi(y)}{dy}|_{y=b} = 0 \tag{2.88}$$

The method of virtual work needs to be used to find the buckling load and wavelength under clamped boundary conditions. Now, recall that the coefficients in the solution equations (2.84) and (2.85) are given by

$$\overline{\Gamma}_1 = \frac{1}{\overline{B}}(2\overline{C}\frac{\overline{\psi}_2}{\overline{\psi}_1} - 4\overline{F}\frac{\overline{\psi}_4}{\overline{\psi}_1} + N_{cr}), \overline{\Gamma}_2 = \frac{1}{\overline{B}}(\overline{D}\frac{\overline{\psi}_3}{\overline{\psi}_1} + k), \overline{\Gamma}'_2 = \frac{\overline{D}}{\overline{B}}\frac{\overline{\psi}_3}{\overline{\psi}_1} \tag{2.89}$$

For the function $\psi(y) = \sin^2\frac{\pi y}{b} = \sin^2\mu y$, where $\mu = \frac{\pi}{b}$, one finds

$$\overline{\psi}_1 = \frac{3b}{8},\ \overline{\psi}_2 = -\frac{\pi^2}{2b} = ,\ \overline{\psi}_3 = \frac{2\pi^4}{b^3},\ \overline{\psi}_4 = \frac{\pi^2}{2b} \tag{2.90}$$

and hence for a plate of the isotropic elastic material, the above coefficients become

$$\overline{\Gamma}_1 = (\frac{N_{cr}}{D} - \frac{8}{3}\mu^2),\ \overline{\Gamma}_2 = (\frac{16}{3}\mu^4 + \frac{k}{D}),\ \overline{\Gamma}'_2 = \frac{16}{3}\mu^4 \tag{2.91}$$

Using these coefficients for determining c_1, d_1 and c_2, d_2 for substituting in into Eqs. (2.63) and (2.64) and carrying out the iterative numerical procedure outlined in Section 2.6, one can arrive at the solution of the critical buckling stresses and the corresponding wavelengths, see Table 2.2.

The results in Table 2.2 are analogous to the case of simply supported plates. The buckling loads and the wavelengths vary with the foundation modulus in the same way.

The buckling load of a long clamped plates with no foundation corresponds to $\lambda = 7.285$, When the foundation is rigid the value of the buckling coefficient is maximum, $\lambda = 10.362$, which represents an increase of 42%. Variation of the buckling load coefficient λ versus foundation stiffness parameter α was shown in Fig. 2-4. The variation of the wavelength to width ratio ζ/b versus foundation stiffness parameter α is shown in Fig. 2-7.

It must be realized that whereas the solution for the simply supported plates was exact, that for the clamped plate is based on an assumed mode shape in the y direction. The latter is therefore an approximate solution, the goodness of which cannot be ascertained exactly. However on physical grounds, the results should be accurate enough, since the assumed mode shape is quite realistic.

Table 2.2 λ, ζ and ξ for elastic infinitely long, clamped plates resting on different tensionless foundations

	$\alpha = 0$	$\alpha = 1.0$	$\alpha = 1000$	$\alpha = 1.0 \times 10^5$	$\alpha = \infty$
λ	7.285	7.483	10.229	10.362	10.362
ζ/b	0.5	0.320	0.075	0.024	0
ξ/b	0.5	0.339	0.467	0.536	0.570

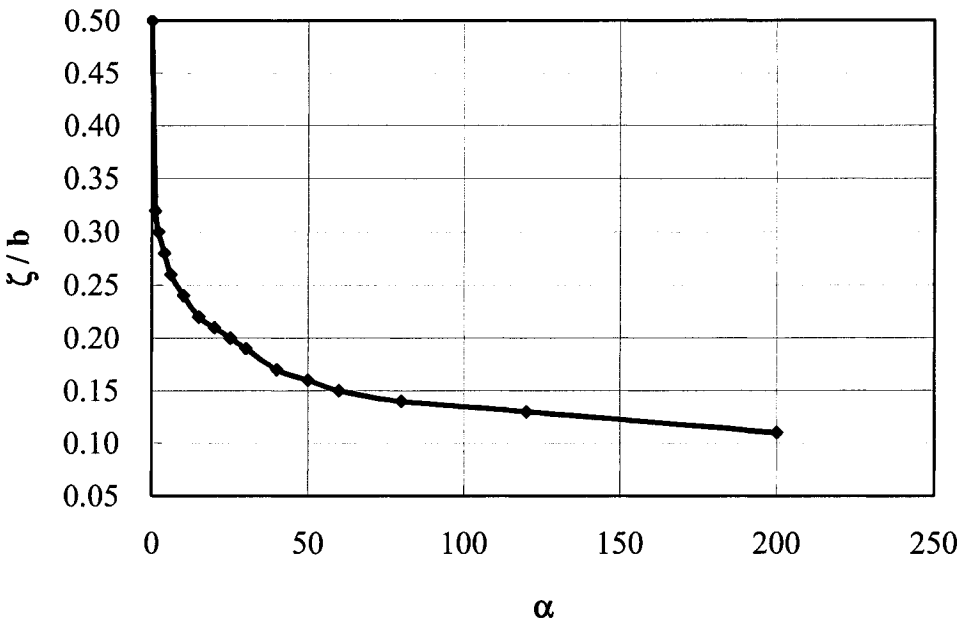

Fig. 2-7 Wavelength to width ratio - foundation stiffness parameter curves with clamped unloaded edges

Chapter 3

Plastic Buckling of Infinitely Long Plates Resting on Elastic Foundations

This chapter is concerned with the plastic buckling of infinitely long plates on elastic foundations. The main difference with the preceding chapter is that now the material moduli are those for an elastic-plastic, strain-hardening material. Aluminum is a typical example of such material, and also some types of steel which do not exhibit a yield plateau like mild steel, but have a rising strain-hardening behaviour. The kinematic assumptions made here are identical to those in the previous chapter. Hence the equations of equilibrium are identical, and so is the virtual work expression.

3.1 Constitutive relations of the plasticity theories

The following discussion is elementary and restricted to the purpose of this thesis. The reader may consult standard books on the theory of plasticity, notably the one by Hill [21] for detailed discussions and explanations.

The constitutive relations needed here for the present bifurcation analyses are of the incremental type. Given a present state of deformation, with stresses $\{\sigma^o\}$ and strains $\{\epsilon^o\}$, they relate the increments in stresses $\{d\sigma\}$to the increments in strains $\{d\epsilon\}$, i.e.,

$$\{d\sigma\}=[D]\{d\epsilon\} \tag{3.1}$$

where $[D]$ is the matrix of elastic/plastic moduli. The matrix $[D]$ incorporates the postulated plastic behaviour of the material, and generally depends on the existing stresses $\{\sigma^o\}$ and strains $\{\epsilon^o\}$. There are two competing theories of plasticity which are simple, and therefore most often used. They are called the J_2 incremental and J_2 deformation theories of plasticity. They both incorporate the following observed and experimentally corroborated behaviour of metals. First, they satisfy the condition of zero plastic volume change in recognition of the fact that, for metals, plasticity arises due to

slip displacements of metal crystals over slip planes. Secondly, they obey the von Mises, or alternatively, the J_2 yield condition :

$$\sigma_e = \sqrt{3J_2} = \sigma'_Y(\varepsilon_P) \tag{3.2}$$

This condition says that, potentially, a plastic deformation is possible if the current stress point, typified by $\sigma_e = \sqrt{3J_2}$ for a general state of stress, lies on the current yield surface. σ_e is called the von Mises equivalent stress. This yield surface depends on the total plastic strain ε_P accumulated during previous history of plastic straining. The yield surface expands uniformly in the stress space with increasing ε_P. This behaviour, valid for small strains, is called isotropic hardening. An increment of stress when the stress point (before the increment) is situated on the yield surface will result in $d\sigma_e = \frac{3}{2}\frac{dJ_2}{\sigma_e}$. If then, $dJ_2 > 0$ there is loading, i.e. there is further plastic deformation. If $dJ_2 = 0$, there is neutral loading in the sense that although no plastic deformation takes place, the material remains in the yield state by virtue of the fact that the stress point is still on the yield surface, and there is possibility of plastic increments of strain for a second increment of stress. When however, $dJ_2 < 0$, there is unloading. The stress point is no longer on the yield surface (it has come inside) and small enough increments of stresses will only produce elastic strains.

The incremental theory postulates relations between the deviatoric stress $s_{ij} = \sigma_{ij} - \frac{\sigma_{kk}}{3}\delta_{ij}$ and the plastic strain increments. The elastic strain increments are related to the stress increments by the standard elastic law for plates. Thus,

$$\{d\epsilon^P\} = h\, dJ_2\, \{s\},\ \{d\epsilon^E\} = [C_E]\{d\sigma\} \tag{3.3}$$

where, h is the hardening parameter related to the position of the stress point on the uniaxial stress-strain curve of the material, and $[C_E]$ is the standard compliance matrix for linear isotropic elastic behaviour. Under the small strain assumption, the total strain increments are taken to be the sum of the elastic and plastic parts. The combined relations may be expressed as

$$\{d\epsilon\} = [C_t]\{d\sigma\},\ \text{or by inverting them as } \{d\sigma\} = [D_t]\{d\epsilon\} \tag{3.4}$$

where $[C_t]$ denotes the incremental compliance matrix, and $[D_t]$ stands for the incremental moduli matrix. It is the inverted form which is needed in the further development of the theory.

The deformation theory postulates relations between the deviatoric stress $s_{ij} = \sigma_{ij} - \frac{\sigma_{kk}}{3}\delta_{ij}$ and the total plastic strains. The elastic strains are related to the stress by the standard elastic law for plates. Thus,

$$\{\epsilon^P\} = \varphi\{s\},\ \{\epsilon^E\} = [C_E]\{\sigma\} \tag{3.5}$$

where now φ is the hardening parameter related to the position of the stress point on the uniaxial stress-strain curve of the material, and $[C_E]$ is the same matrix as earlier. The total strains are taken to be the sum of the elastic and plastic parts. The combined relations may be expressed as

$$\{\epsilon\} = [C_s]\{\sigma\},\ \text{or by inverting them as}\ \{\sigma\} = [D_s]\{\epsilon\} \tag{3.6}$$

where $[C_s]$ denotes the elastic/plastic compliance matrix, and $[D_s]$ is the inverse of $[C_s]$ and may be called the matrix of the secant moduli.

The difference between the incremental theory and the deformation theory is now clear. While the former provides a relation between stress and strain increments, the latter postulates a relation between the total quantities. The deformation theory is therefore like a nonlinear elasticity theory with stress dependent moduli. The incremental theory on the other hand is history dependent and employs the notion of loading and unloading. The two theories however become identical if the loading is proportional in that $d\sigma_{ij} = \alpha\ \sigma_{ij}$. Based on experimental and theoretical considerations, the incremental theory is considered a correct theory of plasticity. However, its application is more difficult. Therefore, despite its weak foundations the deformation theory continues to be used because of its relative simplicity. Moreover, for bifurcation problems, especially of plane plates, the bifurcation loads predicted by the incremental theory are sometimes absurdly higher than the experimental values. Paradoxically, the bifurcation loads predicted by the deformation theory for plane plates are in good and conservative agreement with the test results, and also invariably lower than the bifurcation loads from the incremental theory [22]. Therefore from a practical point of view it is the deformation theory buckling loads

which should be used, like in the present work. The incremental theory is known to be very imperfection sensitive, and hence the maximum loads computed by the incremental theory can be made to agree with the experimental loads if a realistic imperfection growth analysis can be carried out. However, this latter procedure is time consuming, and gives uncertain answers depending upon the amplitudes of the imperfections, and is usually not recommended.

3.2 Constitutive relations for a plastic bifurcation analysis

Now, for a bifurcation analysis, one needs incremental relations, even for the deformation theory. In buckling of the axially stressed plates, the state of stress changes suddenly from a uniaxial one to a multiaxial state, with increments in stress and strain occurring in other directions due to buckling. The needed incremental relations for the deformation theory are obtained by differentiating the total relations indicated above. Without further going into details, it can be said that the applicable stress strain relations can be expressed as [10, 25]

$\{d\sigma\} = [D]\{d\epsilon\}$ or explicitly as

$$d\sigma_{xx} = B' d\epsilon_{xx} + C' d\epsilon_{yy},\ d\sigma_{yy} = C' d\epsilon_{xx} + D' d\epsilon_{yy},\ d\sigma_{xy} = 2F'\, d\epsilon_{xy} \tag{3.7}$$

where it can be shown that

$$B' = \frac{E(\,g + 3e + 3)}{g(5 + 3\,e - 4\nu) - (1 - 2\nu)^2}$$

$$C' = \frac{2E\,(g - 1 + 2\nu)}{g(5 + 3\,e - 4\nu) - (1 - 2\nu)^2}$$

$$D' = \frac{4g}{g(5 + 3\,e - 4\nu) - (1 - 2\nu)^2}$$

$$F' = \frac{E}{2 + 2\nu + 3e} \tag{3.8}$$

and where in the above

$$e = \frac{E}{E_s} - 1,\ g = \frac{E}{E_t} \tag{3.9}$$

These two parameters e and g are found from the uniaxial stress strain curve of the material at the stress level equal to the applied axial stress. E_s is the secant modulus at this level, and E_t is the corresponding tangent modulus.

The above relations, valid for the deformation theory, can be specialized to those for the incremental theory by putting $e = 0$ in the above definitions of the moduli. Furthermore, putting $g = 1$, and $e = 0$ results in the relations for the elastic behaviour.

It is now convenient to change the notation slightly. From now on, the increments in strain and stress due to buckling will be denoted by $\epsilon_{xx},\ \epsilon_{yy}.\ \epsilon_{xy}$ and $\sigma_{xx}, \sigma_{yy}.\ \sigma_{xy}$. Thus, the above relations will read as

$$\sigma_{xx} = B'\epsilon_{xx} + C'\epsilon_{yy},\ \sigma_{yy} = C'\epsilon_{xx} + D'\epsilon_{yy},\ \sigma_{xy} = 2\,F'\,\epsilon_{xy} \tag{3.10}$$

with exactly the same meaning for the moduli as above.

One may now recall the Kirchhoff kinematic hypothesis to connect the buckling strains to buckling deflection $w(x,\ y)$ as

$$\epsilon_{xx} = -\,z\,\frac{\partial^2 w}{\partial x^2},\ \epsilon_{yy} = -\,z\,\frac{\partial^2 w}{\partial y^2}, \epsilon_{xy} = -\,z\,\frac{\partial^2 w}{\partial x \partial y}, \tag{3.11}$$

In accordance with Shanley's concept of plastic bifurcation occurring under increasing load [23, 24], so that the plastic strains increase over the entire thickness of the plate, the moduli are those of loading, and hence the stresses are

$$\sigma_{xx} = -\,z(B'\,\frac{\partial^2 w}{\partial x^2} + C'\frac{\partial^2 w}{\partial y^2}),\ \sigma_{yy} = -\,z(C'\,\frac{\partial^2 w}{\partial x^2} + D'\frac{\partial^2 w}{\partial y^2}),\ \sigma_{xy} = -\,2zF'\frac{\partial^2 w}{\partial x \partial y} \tag{3.12}$$

The moment stress resultants due to buckling are then

$$M_{xx} = \int_{-t/2}^{t/2} z\,\sigma_{xx}dz = -\,\frac{t^3}{12}\,(B'\,\frac{\partial^2 w}{\partial x^2} + C'\,\frac{\partial^2 w}{\partial y^2})$$

$$M_{yy} = \int_{-t/2}^{t/2} z\,\sigma_{yy} dz = \; - \; - \frac{t^3}{12}\,(C'\,\frac{\partial^2 w}{\partial x^2} + D'\,\frac{\partial^2 w}{\partial y^2})$$

$$M_{xy} = \int_{-t/2}^{t/2} z\,\sigma_{xy} dz = \; - \frac{t^3}{12}(2F'\frac{\partial^2 w}{\partial x \partial y})$$

(3.13)

3.3 Equations for buckling loads and wavelengths by the equilibrium method

A procedure similar to the elastic case is now followed to derive the exact buckling conditions for a plate simply supported along the longitudinal edges, $y = 0,\ b$.

The applicable equilibrium equations, independent of the material behaviour, are

$$\frac{\partial^2 M_x}{\partial x^2} + 2\,\frac{\partial^2 M_{xy}}{\partial x \partial y} + \frac{\partial^2 M_y}{\partial y^2} - N_{\rm cr}\frac{\partial^2 w}{\partial x^2} - kw = 0 \tag{3.14}$$

in the contact zones, and

$$\frac{\partial^2 M_x}{\partial x^2} + 2\,\frac{\partial^2 M_{xy}}{\partial x \partial y} + \frac{\partial^2 M_y}{\partial y^2} - N_{\rm cr}\frac{\partial^2 w}{\partial x^2} = 0 \tag{3.15}$$

in the no-contact zones.

Substitution of the expressions in terms of the curvatures transforms (3.14) and (3.15) to

$$B'\,\frac{\partial^4 w}{\partial x^4} + 2(C' + 2F')\,\frac{\partial^4 w}{\partial x^2 \partial y^2} + D'\,\frac{\partial^4 w}{\partial y^4} + \frac{12\,N_{cr}}{t^3}\,\frac{\partial^2 w}{\partial x^2} + \frac{12\,k}{t^3}\,w = 0 \tag{3.16}$$

and

$$B'\,\frac{\partial^4 w}{\partial x^4} + 2(C' + 2F')\,\frac{\partial^4 w}{\partial x^2 \partial y^2} + D'\,\frac{\partial^4 w}{\partial y^4} + \frac{12\,N_{cr}}{t^3}\,\frac{\partial^2 w}{\partial x^2} = 0 \tag{3.17}$$

3.3.1 Equations for buckling displacements in the contact and no-contact regions

The boundary conditions of simply supports at $y = 0,\ b$, admits a product solution in the form, in the contact zones, as

$$w_1(x_1,\ y) = \phi_1(x_1) \sin \frac{n\pi y}{b} = \phi_1(x_1) \sin \mu y \tag{3.18}$$

where n is the number of half waves in the y direction. As previously, $n = 1$ corresponds to the critical buckling mode, and hence $\mu = \pi/b$. Substitution of this solution in the differential equation for the contact zones results in

$$\frac{d^4\phi_1}{dx_1^4} + (\frac{12\,N_{cr}}{B't^3} - \mu^2 \frac{2C' + 4F'}{B'}) \frac{d^2\phi_1}{dx_1^2} + (\frac{D'}{B'}\mu^4 + \frac{12\,k}{B't^3})\,\phi_1 = 0 \tag{3.19}$$

By setting

$$\Gamma_3 = \frac{12\,N_{cr}}{B't^3} - \mu^2 \frac{2C' + 4F'}{B'}\,,\ \Gamma_4 = \frac{D'}{B'}\mu^4 + \frac{12\,k}{B't^3}\,, \tag{3.20}$$

the above can be written as

$$\frac{d^4\phi_1}{dx_1^4} + \Gamma_3 \frac{d^2\phi_1}{dx_1^2} + \Gamma_4\,\phi_1 = 0 \tag{3.21}$$

Similarly in the no-contact zones by denoting the displacement as

$$w_2(x_2,\ y) = \phi_2(x_2) \sin \frac{\pi y}{b} = \phi_2(x_2) \sin \mu y \tag{3.22}$$

it is found that $\phi_2(x_2)$ must satisfy

$$\frac{d^4\phi_2}{dx_2^4} + (\frac{12\,N_{cr}}{B't^3} - \mu^2 \frac{2C' + 4F'}{B'}) \frac{d^2\phi_2}{dx_2^2} + \frac{D'}{B'}\mu^4\,\phi_2 = 0 \tag{3.23}$$

Introducing the symbols

$$\Gamma'_3 = \Gamma_3 = \frac{12\,N_{cr}}{B't^3} - \mu^2\frac{2C' + 4F'}{B'}, \text{ and } \Gamma'_4 = \frac{D'}{B'}\mu^4 \tag{3.24}$$

the above equation can be written as

$$\frac{d^4\phi_2}{dx_2^4} + \Gamma'_3\frac{d^2\phi_2}{dx_2^2} + \Gamma'_4\phi_2 = 0 \tag{3.25}$$

3.3.2 Derivation of the buckling equations

The solution form of the functions $\phi_1(x_1)$ is exactly the same as that obtained for the elastic case, namely

$$\phi_1(x_1) = \frac{A}{c_1}\{\sinh(c_1x_1)\sin(d_1x_1) - \tanh(c_1\zeta)\tan(d_1\zeta)\cosh(c_1x_1)\cos(d_1x_1)\} \tag{2.26}$$

except that c_1 and d_1 are obtained from the present definitions of Γ_3 and Γ_4 for the plastic case (rather than Γ_1 and Γ_2 of the elastic case).

Likewise, for the no-contact zone $\phi_2(x_2)$ is of the same as in the elastic case, namely

$$\phi_2(x_2) = \frac{B}{c_2}\{\sinh(c_2x_2)\sin(d_2x_1) - \tanh(c_2\xi)\tan(d_2\xi)\cosh(c_2x_1)\cos(d_2x_1)\} \tag{2.40}$$

except that c_2 and d_2 are obtained from the present definitions of Γ'_3 and Γ'_4 for the plastic case.

As mentioned in Section 2.3 as well as 2.4, previously, the product solution ensures that the matching conditions remain the same, which at the common edges of the contact and no-contact zones require equality of the functions to zero, and equality of the first, second, and third derivatives. The two buckling equations are of the same form as for the elastic case, repeated here for convenience

$$\text{Eq1} = \frac{1}{c_1d_1}\frac{\{c_1\sin(2d_1\zeta)+d_1\sinh(2c_1\zeta)\}}{\{\cos(2d_1\zeta)+\cosh(2c_1\zeta)\}} - \frac{1}{c_2d_2}\{\frac{c_2\sin(2d_2\xi)+d_2\sinh(2c_2\xi)}{\cos(2d_2\xi)+\cosh(2c_2\xi)}\} = 0 \tag{2.63}$$

$$\text{Eq2} = \frac{1}{c_1 d_1} \frac{\{c_1 \sin(2d_1\zeta) + d_1 \sinh(2c_1\zeta)\}}{\{(c_1^2 - 3\,d_1^2)\sin(2d_1\zeta) + \frac{d_1}{c_1}(3c_1^2 - d_1^2)\sinh(2c_1\zeta)\}} +$$
$$- \frac{1}{c_2 d_2} \frac{\{c_2 \sin(2d_2\xi) + d_2 \sinh(2c_2\xi)\}}{\{(c_2^2 - 3\,d_2^2)\sin(2d_2\xi) + \frac{d_2}{c_2}(3c_2^2 - d_2^2)\sinh(2c_2\xi)\}} = 0 \tag{2.64}$$

Therefore, the method of solving Eqs. (2.63) and (2.64) explained previously in Chapter 2 can also be applied to the plastic buckling equations. However, in solving these equations, one must remember that the moduli to be used here are stress dependent (and not constants as was the case with elastic buckling).

3.4 Equations for buckling loads and wavelengths by the method of virtual work

There is no need to repeat the virtual work method introduced in the last Chapter. The method was developed using a general form of the constitutive relations with $\bar{B}$, $\bar{C}$, $\bar{D}$, and $\bar{F}$ as symbols for the moduli. Here these moduli are identified as the elastic-plastic moduli B', C', D', F' defined by Eq. (3.8).

The forms of the deflections are taken as

$$w_1(x, y) = \phi_1(x_1)\,\psi(y), \tag{3.26}$$

$$w_2(x, y) = \phi_2(x_2)\,\psi(y) \tag{3.27}$$

Thus leads to the differential equation for the contact zones

$$\frac{d^4\phi_1}{dx_1^4} + \bar{\Gamma}_3 \frac{d^2\phi_1}{dx_1^2} + \bar{\Gamma}_4\,\phi_1 = 0 \tag{3.28}$$

where

$$\bar{\Gamma}_3 = \frac{2C'}{B'}\frac{\bar{\psi}_2}{\bar{\psi}_1} - \frac{4F'}{B'}\frac{\bar{\psi}_4}{\bar{\psi}_1} + \frac{N_{cr}}{B'},\ \bar{\Gamma}_4 = \frac{D'}{B'}\frac{\bar{\psi}_3}{\bar{\psi}_1} + \frac{k}{B'} \tag{3.29}$$

and the equation for the no-contact zones

$$\frac{d^4\phi_2}{dx_2^4} + \overline{\Gamma}'_3 \frac{d^2\phi_2}{dx_2^2} + \overline{\Gamma}'_4 \phi_2 = 0 \tag{3.30}$$

where

$$\overline{\Gamma}'_3 = \overline{\Gamma}_3 = \frac{2C'}{B'}\frac{\bar{\psi}_2}{\bar{\psi}_1} - \frac{4F'}{B'}\frac{\bar{\psi}_4}{\bar{\psi}_1} + \frac{N_{cr}}{B'}, \; \overline{\Gamma}'_4 = \frac{D'}{B'}\frac{\bar{\psi}_3}{\bar{\psi}_1} \tag{3.31}$$

For a plate clamped on the edges $y = 0,\ b,$ the mode form $\psi(y)$ satisfying the condition of zero deflections and zero slopes is assumed to be the same as for the elastic case, as

$$\psi(y) = \sin^2 \frac{\pi y}{b} = \sin^2 \mu y\,, \tag{3.32}$$

from the equation (2.73), one then finds

$$\bar{\psi}_1 = \frac{3b}{8},\ \bar{\psi}_2 = -\frac{\pi^2}{2b},\ \bar{\psi}_3 = \frac{2\pi^4}{b^3},\ \bar{\psi}_4 = \frac{\pi^2}{2b} \tag{2.81}$$

And hence for a plate of the isotropic elastic material, the above coefficients become

$$\overline{\Gamma}_3 = \overline{\Gamma}'_3 = (\frac{N_{cr}}{D} - \frac{8}{3}\mu^2),\ \overline{\Gamma}_4 = (\frac{16}{3}\mu^4 + \frac{k}{D}),\ \overline{\Gamma}'_4 = \frac{16}{3}\mu^4 \tag{3.33}$$

The form of the solution functions $\phi_1(x_1)$ and $\phi_2(x_2)$ is the same in Section 2.5. The matching conditions also remain unchanged. Hence the forms of the two buckling equations are the same as Eqs. (2.63) and (2.64) except that the moduli are stress dependent, and the quantities $c_1,\ d_1,\ c_2,\ d_2$ have to be found from the present definition of $\overline{\Gamma}_3,\ \overline{\Gamma}_4, \overline{\Gamma}'_3,\ \overline{\Gamma}'_4$.

3.5 Buckling loads and wavelengths for simply supported plates

The plastic buckling problem is a bit more complicated than the elastic one. The reason is that the tangent and secant moduli required in the calculations are dependent on the stress-strain curve of the plate material, and on the critical stress at which these moduli

must be computed. Therefore, a part of the input data is the uniaxial stress-strain curve. Here, as an example, the plate material is taken as an Aluminum alloy, 24S-T3. For this alloy one has $E = 76,535\,\text{MPa}$, $\nu = 0.32$, and the 0.2% proof stress (equivalent to the yield stress) $\sigma_y = 300\,\text{MPa}$. The following Ramberg-Osgood function is suitable [25, 26] for expressing strain as a function of stress:

$$\varepsilon = \frac{\sigma_{cr}}{76,535} + 0.002\,(\frac{\sigma_{cr}}{300})^7 \tag{3.34}$$

The $\varepsilon - \sigma$ graph of this function is shown in Fig. 3-1.

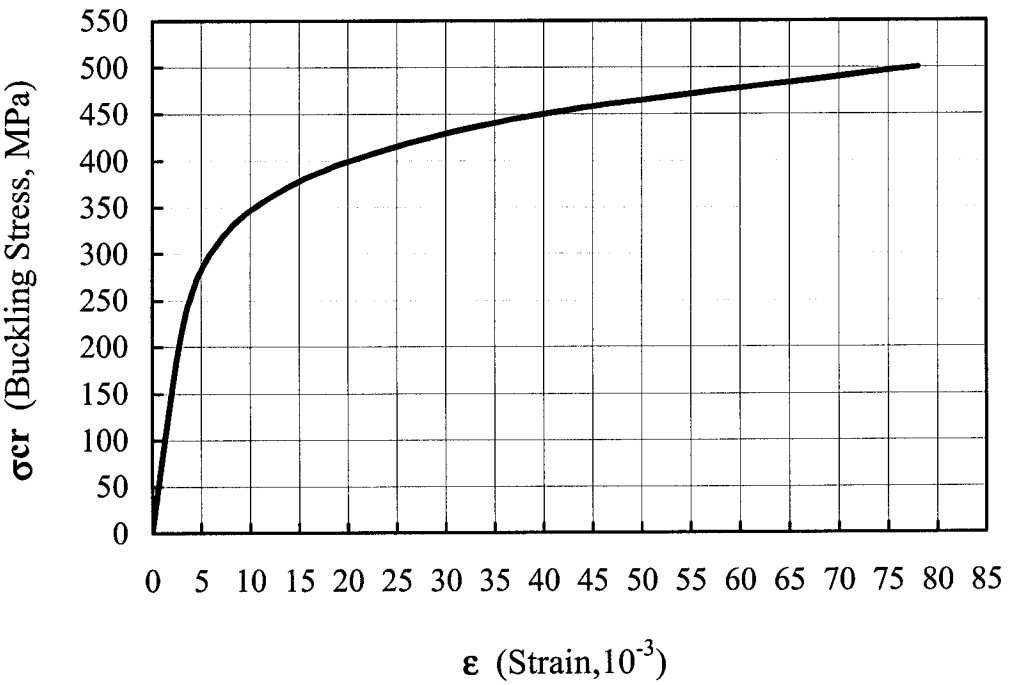

Fig. 3-1 Uniaxial stress-strain curve for Aluminum alloy 24S - T3

By using Eqs. (2.63) and (2.64) through the *Mathematica* software and employing both the deformation and the incremental theories, one finds a set of results of λ, ζ/b and ξ/b for an infinitely long plate simply supported on longitudinal edges, resting on a one-way elastic foundation, and loaded by uniform compressive force in x direction. The results are mathematically exact unlike those for the clamped plate (to be discussed shortly)

which are based on an assumed but reasonable mode shape. These results are shown in Table 3.1 for the deformation theory, and in Table 3.2 for the incremental theory.

Table 3.1 λ, ζ and ξ for an infinitely long simply supported Al alloy 24S - T3 plate resting on elastic one-way foundations with different foundation parameter α ($b/t = 25$, Deformation theory)

	$\alpha = 0$	$\alpha = 1.0$	$\alpha = 1000$	$\alpha = 1.0 \times 10^5$	$\alpha = \infty$
λ	2.602	2.672	2.797	2.798	2.798
ζ/b	0.5	0.320	0.056	0.018	0
ξ/b	0.5	0.446	0.639	0.693	0.707

Table 3.2 λ, ζ and ξ for an infinitely long, simply supported Al alloy 24S - T3 plate resting on elastic one-way foundations with different foundation parameter α ($b/t = 25$, Incremental theory)

	$\alpha = 0$	$\alpha = 1.0$	$\alpha = 1000$	$\alpha = 1.0 \times 10^5$	$\alpha = \infty$
λ	3.363	3.524	3.978	3.986	3.986
ζ/b	0.5	0.290	0.054	0.017	0
ξ/b	0.5	0.379	0.548	0.599	0.615

These results show that the plate indeed buckles in the plastic range. For $\alpha = 0$, i.e., with no foundations, the buckling loads from the present theory are equal to the ones calculated by Bijlaard [10]. As usual, the bifurcation buckling loads from the incremental theory are significantly higher than the ones predicted by the deformation theory. Also, the buckling loads are affected by the width to thickness b/t ratio. Relatively stockier plates with smaller b/t will undergo plastic buckling.

As expected, the buckling load increases and the contact length decreases with the increase in the foundation modulus. However, the maximum increase in the buckling load is limited to 7.5% for the deformation theory, and 18.5% for the incremental theory. Fig. 3-2 shows the effect of the increase in foundation modulus on the buckling load for the above plate. It is clear from this figure that the maximum increase in buckling load can be realized by relatively soft foundations.

The contact length decreases with the increase in the foundation modulus, as shown in Fig. 3-3 for the deformation theory and in Fig. 3-4 for the incremental theory. Evidently the contact length diminishes rapidly as the foundation modulus is increased. The contact length is about 10% of the width for a considerable range (50-200) of the foundation parameter.

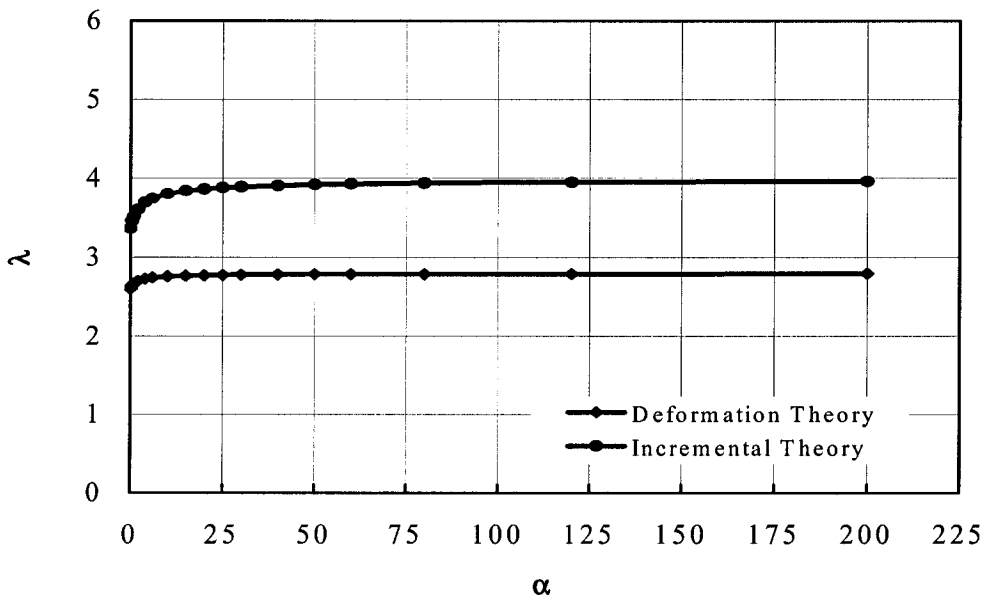

Fig. 3-2 Plastic buckling parameter λ vs. foundation stiffness α for simply supported plates

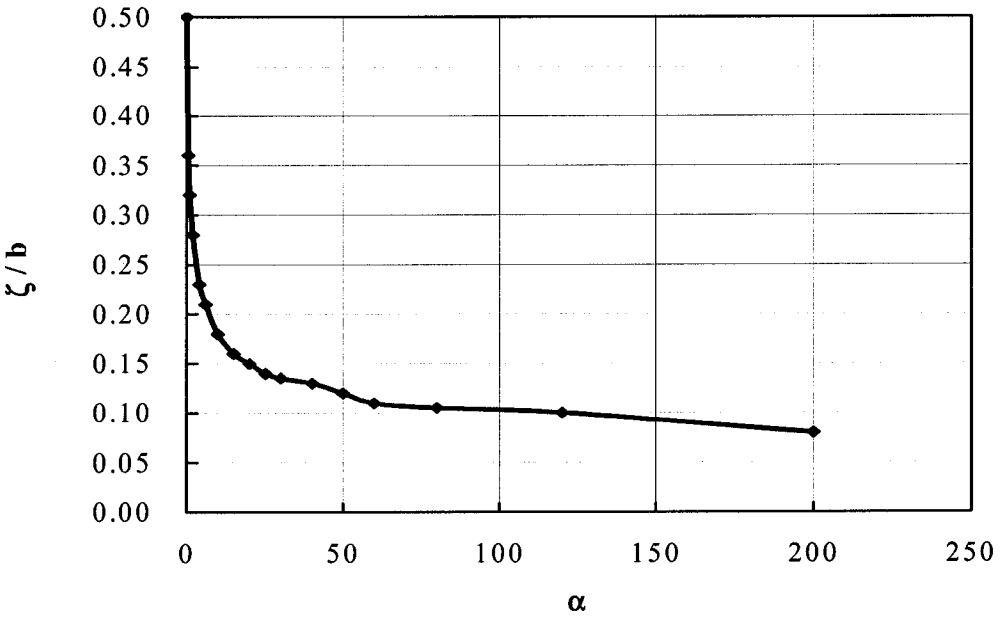

Fig. 3-3 Contact length /plate-width vs. foundation stiffness for simply supported plates; Deformation theory results

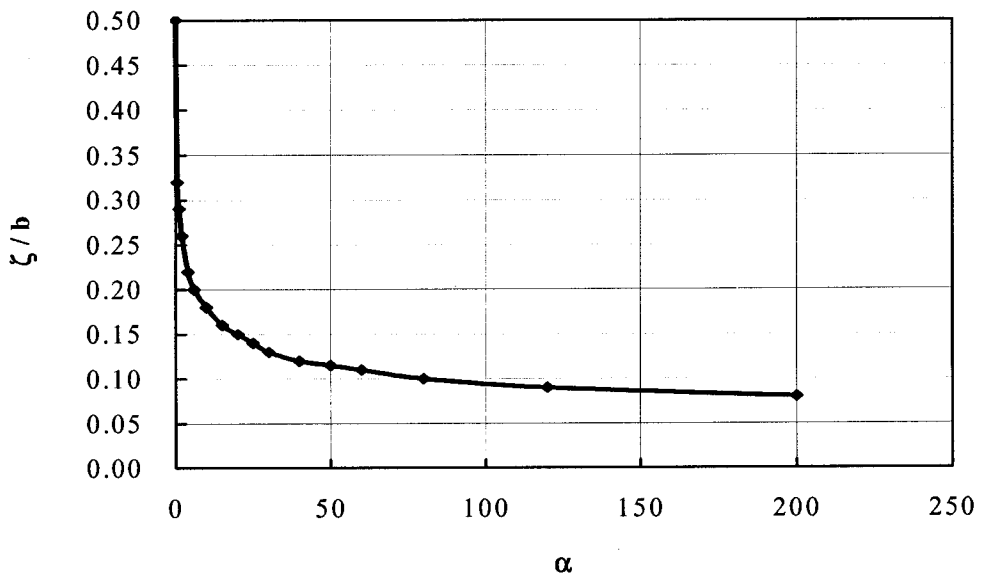

Fig. 3-4 Contact length /plate-width vs. foundation stiffness for simply supported plates; Incremental theory results

3.6 Buckling loads and wavelengths for clamped plates

The plate in this section is clamped along its longitudinal edges and resting on a one-way elastic foundation. Hence equations (2.63) and (2.64) corresponding to the method of virtual work need to be used to obtain the minimum buckling loads and wavelengths. The solution is semi-exact since a reasonable mode shape was assumed in the longitudinal direction to effect the separation of variables. Mathematically, it is not possible to say how good are the results, but physically we may compare them with experiments. The plate material is Aluminum alloy 24S - T3, with a uniaxial stress-strain curve shown previously (Fig. 3-1).

Following the same procedure as in the last section, one obtains a series of results for λ, ζ/b and ξ/b as functions of the foundation stiffness parameter α. These results are determined for both the deformation and the incremental theories. Table 3.3 shows some of these results for the deformation theory, whereas Table 3.4 gives the parallel results for the incremental theory.

Table 3.3 λ, ζ, ξ for an infinitely long, clamped Al alloy 24S-T3 plate resting on one-way elastic foundations for different foundation parameter α ($b/t = 25$, Deformation theory)

	$\alpha = 0$	$\alpha = 1.0$	$\alpha = 1000$	$\alpha = 1.0 \times 10^5$	$\alpha = \infty$
λ	3.033	3.062	3.238	3.242	3.242
ζ/b	0.5	0.240	0.049	0.015	0
ξ/b	0.5	0.270	0.389	0.433	0.451

Table 3.4 λ, ζ, ξ for an infinitely long, clamped Al alloy 24S-T3 plate resting on one-way elastic foundations for different foundation parameter α ($b/t = 25$, Incremental theory)

	$\alpha = 0$	$\alpha = 1.0$	$\alpha = 1000$	$\alpha = 1.0 \times 10^5$	$\alpha = \infty$
λ	5.342	5.440	6.757	8.892	8.897
ζ/b	0.5	0.220	0.053	0.017	0
ξ/b	0.5	0.235	0.330	0.497	0.517

For the deformation theory the maximum increase in the buckling parameter λ for this plate $(b/t - 25)$ is less than 7%. For the incremental theory it is more than 66%. These increases in λ versus foundation parameter α are seen more clearly in Fig. 3-5. The predictions are quite insensitive to stiffness parameter $\alpha > 25$ for the deformation theory and $\alpha > 100$ for the incremental theory

Fig. 3-6 and 3-7 express the variation of the contact length versus the foundation parameter α. The contact length decreases rapidly first as the foundation modulus is increased, but settles down to about 10% of the plate width at $\alpha = 75$.

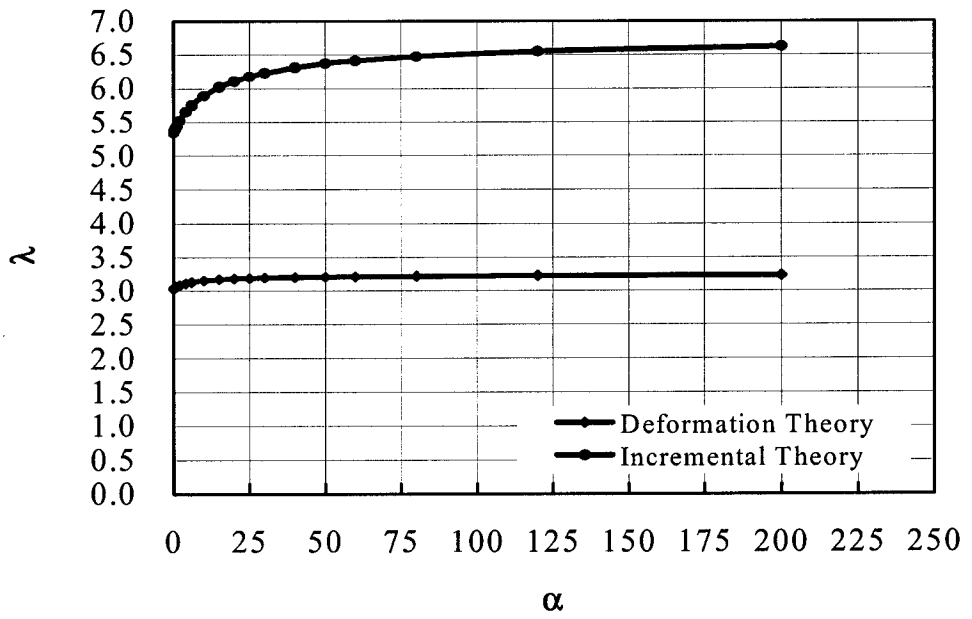

Fig. 3-5 Plastic buckling parameter λ vs. foundation stiffness α for clamped plates

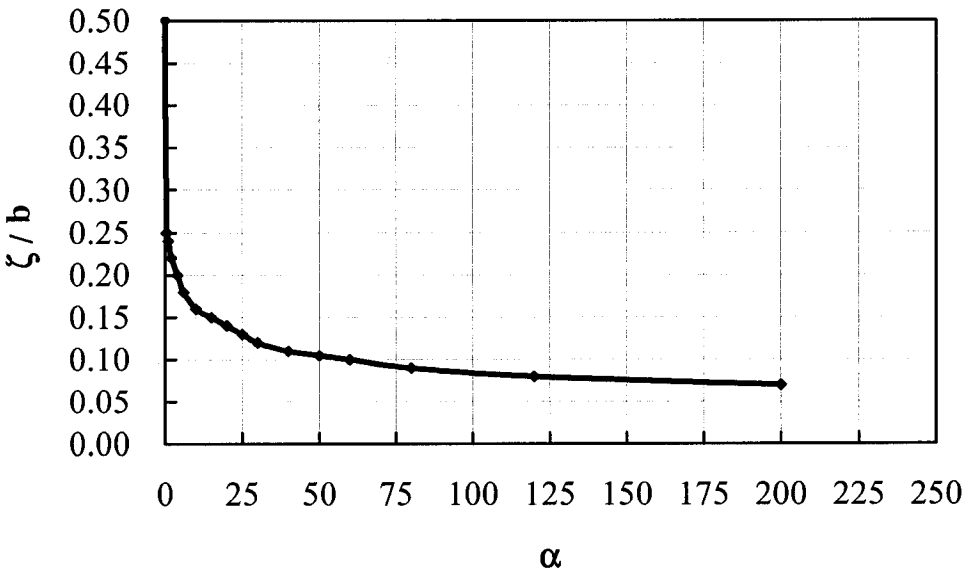

Fig. 3-6 Contact length /plate-width vs. foundation stiffness for clamped plates; Deformation theory results

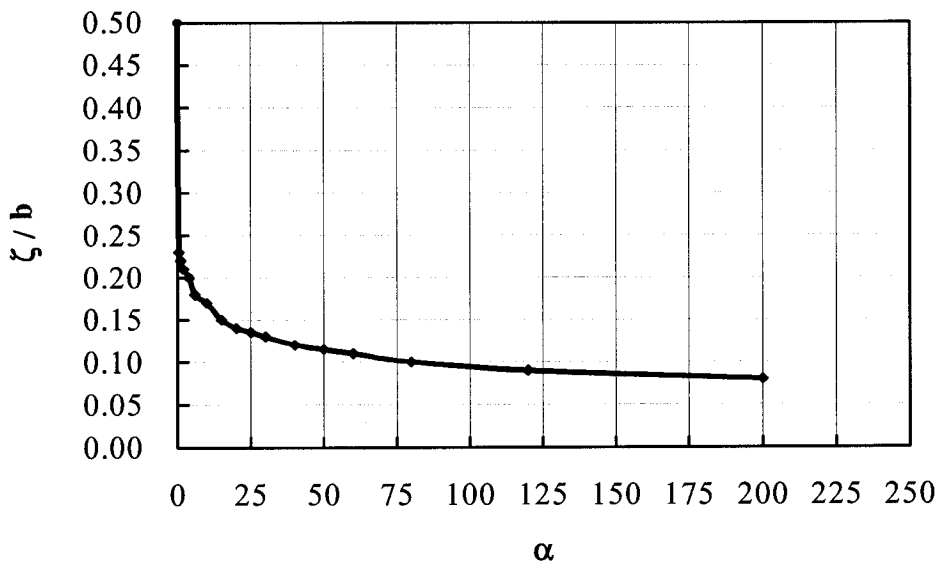

Fig. 3-7 Contact length /plate-width vs. foundation stiffness for clamped plates; Incremental theory results

Chapter 4

Application to Concrete-filled Steel Box Columns, and Verifications with Experiments

This chapter presents applications as well as verifications of the theoretical buckling analyses of the preceding chapter. First, the present theory is employed for calculating the ultimate loads of concrete-filled steel box columns. Then, these theoretical results are verified against available experimental results of other researchers, namely those of Dalin Liu [1] and of Brain Uy, Q. and Q. Liang [5, 6]. Comparison of the theoretical results is also made with the values obtained by using empirical equations of the current design codes of different countries.

4.1 Application to concrete-filled steel box columns

Concrete-filled steel box columns, of square or rectangular shapes, are being used extensively in multi-storey building construction throughout the world [1, 5, 18]. These columns are formed by pouring concrete into fabricated steel-box columns after they have been secured and positioned on site. They are more cost-effective than bare (unfilled) steel columns as well as reinforced concrete columns. The behaviour of the concrete-filled steel box columns is influenced by deformation of both steel and encased concrete.

Numerous experiments conducted in recent years have revealed that typical failure modes of concrete-filled columns are buckling in steel sections and crushing in concrete, see Fig. 4-1. Based on the present theory, the buckling of a steel section is identified with the buckling of the steel plates of the box section, taking into consideration the constraining influence of the in-filled concrete. Consequently, the ultimate strength for concrete-filled box columns is calculated from the buckling load of steel plates, and the maximum capacity in compression of the concrete core. The combined failure load, based upon simultaneous buckling of steel box column plates and crushing of concrete, is expressed as

$$N_T = N_s + N_c = \sigma_{cr} A_s + 0.85\, f'_c A_c \tag{4.1}$$

in which, $N_s = \sigma_{cr} A_s$, is the buckling load of steel box sections, and $N_c = 0.85\, f'_c A_c$ is the maximum concrete capacity in compression. σ_{cr} denotes the critical buckling stress of steel plates unilaterally constrained by the in-filled concrete. The foundation modulus k (also called the normal stiffness) of concrete is generally taken [5] as 23 GPa. This value corresponds to an α around 500, 000 (depending on b/t ratio of the column section). For rectangular columns, the applicable width-to-thickness ratio is the larger one, i.e., b/t as shown in Fig. 4-2. The plates with larger width will buckle first and the corresponding b/t must be used in the formulas to calculate the buckling stress σ_{cr}. A_s is the area of steel section, $A_s = 4bt$ for square sections and $A_s = 2bt + 2ht$ for rectangular sections. f'_c is the strength of test cylinders and A_c equals to the area of the concrete section. The modification factor 0.85 is used to account for the uncertainty between the concrete strength in laboratory and in situ. In the above formula, although the influence of concrete confinement on the steel plates has been accounted for, the confinement effect of steel on the encased concrete is not. This latter effect in a concrete-filled rectangular columns is limited to the corners of the section and is small enough to be omitted [5].

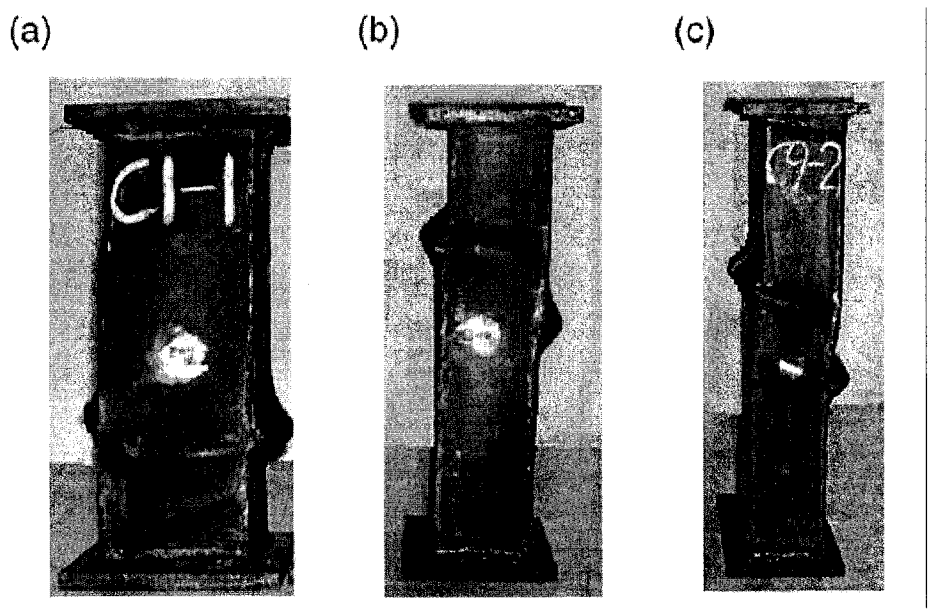

Fig. 4-1 Typical failure modes of concrete-filled box columns [1]

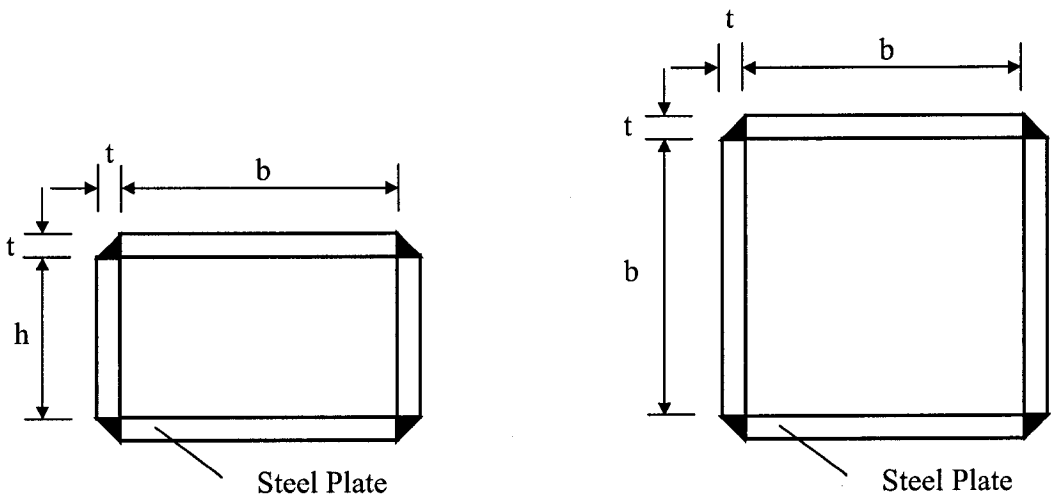

(a) Rectangular Plate (b) Square Plate

Fig. 4-2 Sections of steel box columns

Determination of σ_{cr} in Equation (4.1) is the most important step to calculate the ultimate strength of concrete-filled steel box columns. For determining σ_{cr}, the properties of steel should be ascertained, especially the stress-strain curve in the elastic as well plastic ranges. This stress-strain curve is usually obtained from coupon tests of the steel of the box sections. This curve is then modeled approximately by an analytical expression, expressing strain as a function of stress, $\epsilon = \epsilon(\sigma)$. In the present work, the stress-strain curves are modeled by adopting the well-known Ramburg-Osgood representation [26].

The applicable boundary conditions at the edges of plates, for an un-filled section are taken as simply supported. However, for plates of the concrete-filled sections, the appropriate conditions are those for clamped plates. These assumptions, as depicted in Fig. 4-3, model the actual conditions quite closely.

Although analytical results were presented for both the J_2 incremental and J_2 deformation theories of plasticity, it was found (and it is well known for bare plates) that the bifurcation stress predicted on the basis of the incremental theory is too high compared with the experimental values. On the other hand, the bifurcation stress calculated from the deformation theory matches quite well with experiments, and in fact provides slightly

conservative (i.e., safe) predictions. Therefore as a practical option, the theoretical results of only the deformation theory will be used in this chapter. This is quite acceptable as the deformation theory has been in wide use in engineering practice.

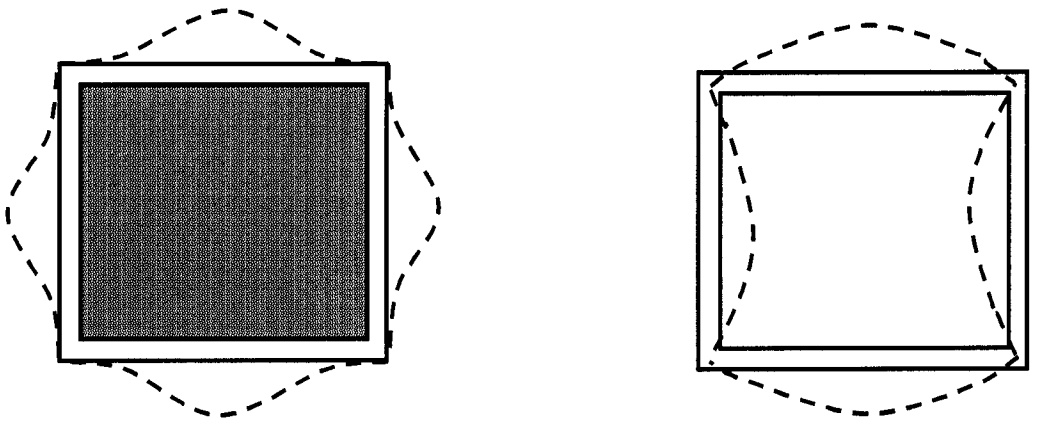

(a) Concrete-filled steel box columns (b) Hollow steel box columns

Fig. 4-3 Buckling modes of steel box columns

In reality, the length of the column is generally much greater than its width. Thus, the plates making up the box column can be considered to be "infinitely" long to fulfill the conditions of the present theory. It is well-known [27] that the buckling load of a plate is not affected by its aspect ratio (length a to width b ratio) if it is greater than 4. In this connection, it is worthwhile to mention the work of Shahwan [4], in which he showed that for axially compressed elastic plates attached to an elastic (Winkler) foundation, their buckling loads varied little with plate's aspect ratio, after it is larger than even one. Figure 4-4, taken from Ref. [4] makes this point very clearly. The graph shows variation of the elastic buckling stress with the aspect ratio, It can be observed that the higher the foundation modulus, the less is the deviation of the buckling stress with that at aspect ratio of unity. The above conclusion is extended here to the plastic buckling of unilaterally constrained plates. Thus, the theory developed for infinitely long plates is suitable for the practical cases of plates of finite lengths.

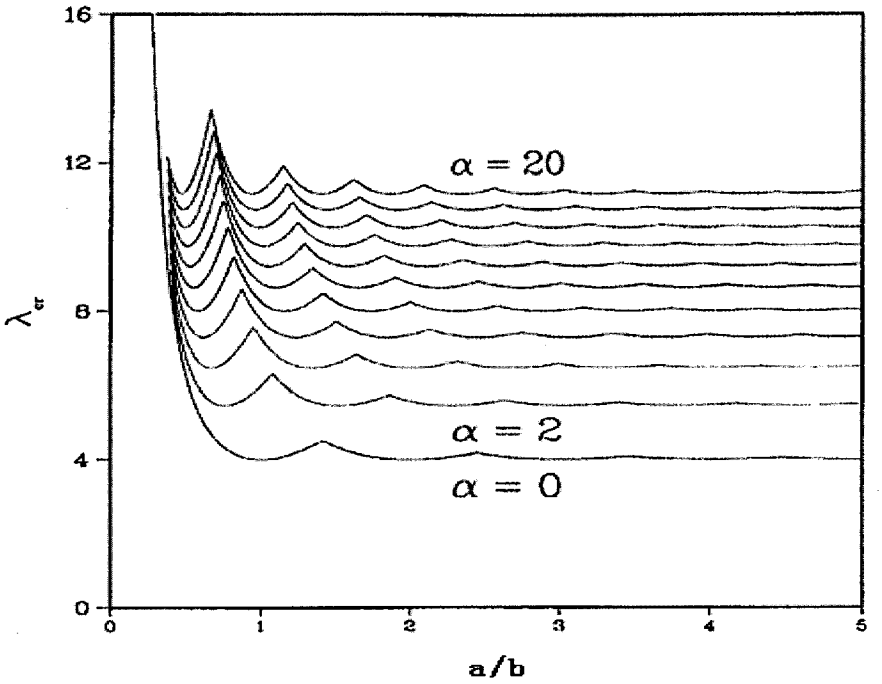

Fig. 4-4 Buckling load coefficient λ_{cr} vs. aspect ratio a/b for simply supported isotropic elastic plates fixed to a foundation of stiffness α [4]

4.2 Verification with experiments

As mentioned before, there are a number of experiments that have been reported in the literature on the strength of concrete-filled steel box columns. These tests employed both the normal strength and high strength steels. Here the theoretical results are compared with the results of the tests which were conducted by Q. Q. Liang *et al.* [5], Brain Uy [6] and Dalin Liu *et al.* [1]. These experiments cover a variety of steel and concrete types, and columns with filled as well as hollow sections, square sections, and rectangular sections.

According to the test data reported by Liang and Uy [5], the stress-strain curve of the steel used by them was approximated by the author as a Ramberg-Osgood curve by the following equation [25]:

$$\epsilon = \frac{\sigma}{E}[1 + \frac{3}{7}(\frac{\sigma}{\sigma_y})^{25}] \tag{4.2}$$

The graphical representation of this equation is shown in Fig. 4-5.

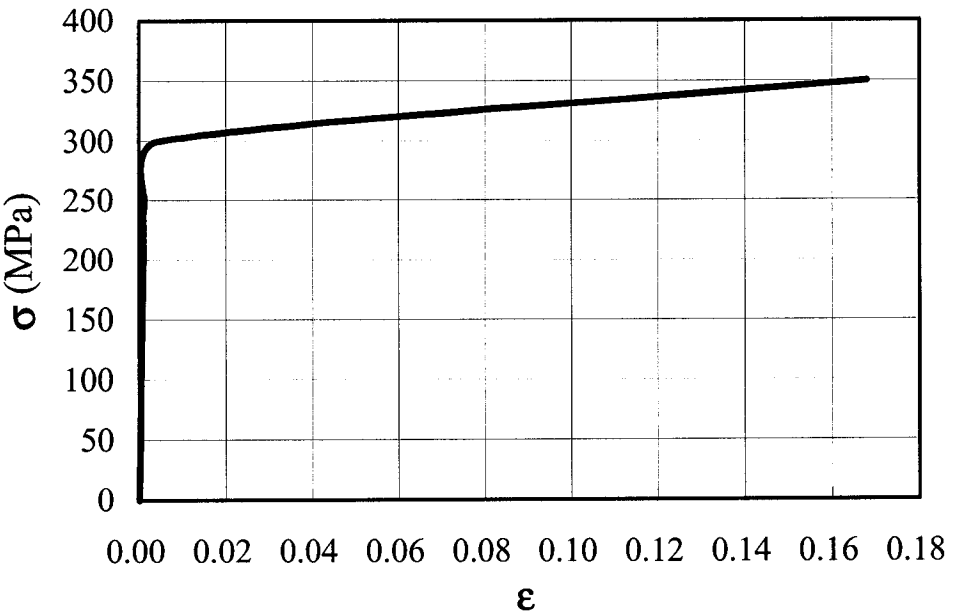

Fig. 4-5 Ramberg- Osgood curve of steel ($\sigma_y = 281$MPa) used in the experiments conducted by Liang and Uy [5]

Similarly, the Ramberg-Osgood curves were derived for the experiments conducted by Uy [6], and by Dalin Liu *et al.* [1] respectively. The curve for the former series of tests [6] was found to be

$$\epsilon = \frac{\sigma}{E} + 0.002\,(\frac{\sigma}{\sigma_y})^{34} \tag{4.3}$$

and for the latter ones [1] as

$$\epsilon = \frac{\sigma}{E} + 0.002\,(\frac{\sigma}{\sigma_y})^{46} \tag{4.4}$$

The graphs of these equations are shown in Fig. 4-6 and 4-7 respectively.

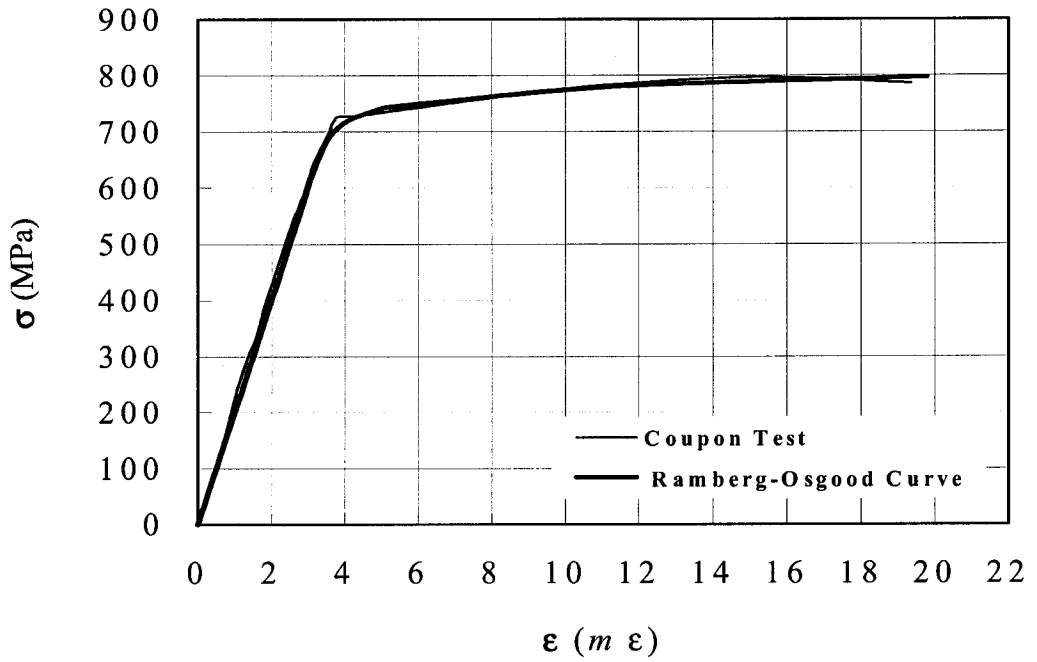

Fig. 4-6 Ramberg-Osgood curve for steel used in the experiment conducted by Uy [6]

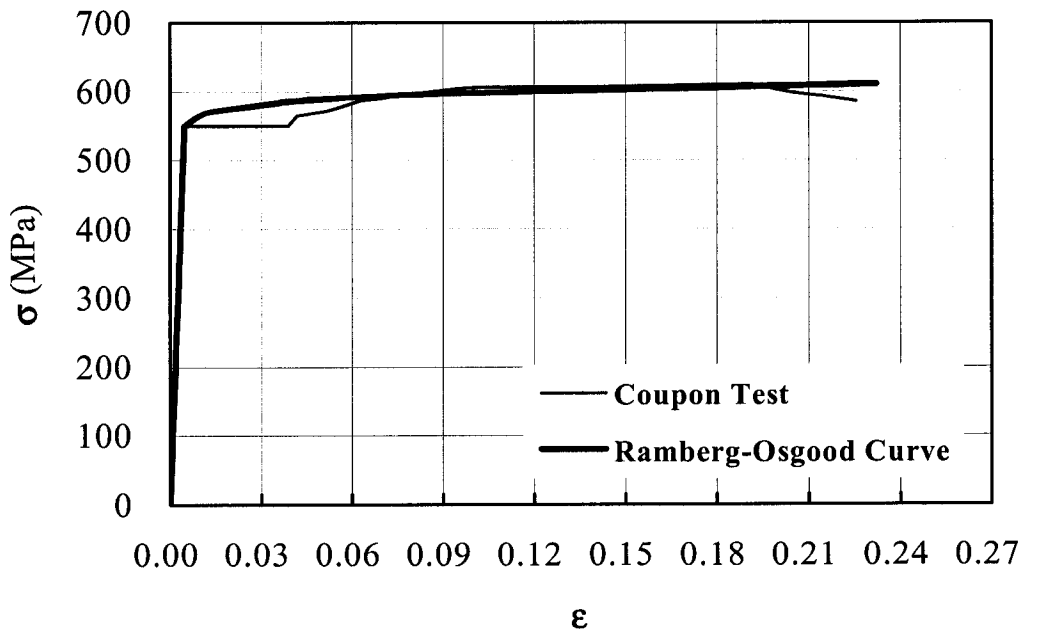

Fig. 4-7 Ramberg-Osgood curve for steel used in the experiment conducted by D. Liu *et al.* [1]

Using the respective Ramberg-Osgood representations, one can determine the secant and tangent moduli as functions of the axial stress. These moduli are needed in the buckling equations of Chapter 3, to determine the buckling stress according to the deformation theory of plasticity. Formula (4.1) can then be used to obtain the theoretically predicted failure load for the individual specimen of each experiments mentioned above. The comparisons between the present theory and each experiment are shown in Table 4.1-4.5.

For the study [5], with data tabulated in Table 4.1, there are six specimens for which all sections are square. The strengths of both the steel and concrete are normal (not high strength). It is found that the results of the presented theory are little lower (i.e., on safe side) than the experimental results, and the differences lie in the range of 0.1% to 12% with an average of 4%. There are three specimens showing nearly the same values between the predictions and tests. Thus, the present theoretical results are in better agreement with the test results than those computed by other researchers by using the finite strip method of analysis; their results are lower than the test results from 2% to 18% with the average of 8%.

The agreement with test results is even better for the experiment reported in [6], see Table 4.2. For 8 specimens, there is a mean difference of only 1% from the experimental results, and three of them are almost the same as the experiments. The exceptions, are the specimens HSS14 and HSS15. The differences for them are quite out of line, which suggests a discrepancy in the reported data. The distinct characteristic in this set of test is that the steel is of the high strength variety. Hence, the comparisons for the cases in [5] and [6] show that the present theory can be used for both high and low strength steel box columns.

For the experiments reported in [1], comparison is made for up to 10 specimens, not only between the theoretical and experimental results but also with the values obtained by using the equations of the design codes of different countries, as shown in Table 4.3 and Table 4.4. The present theoretical results are all on the safe side (i.e. below the experimental values), and can be seen to be more accurate than those calculated by the design formulas of AISC and ACI. However, the results from the equations of EC4 compare quite well with the experiments. In comparison with the test results, the mean values of the calculated results are lower by about 10%, 15%, 14% and 9% for the present theoretical prediction, AISC, ACI, and EC4, respectively. Thus, the results from EC4 appear a little better than the present theory for this series of tests. However, one should

keep in mind the limitation of the EC4 equations. The EC4 formulas are applicable only to the cases where concrete and steel strengths are not greater than 40 MPa and 355 MPa respectively. Hence, in fact, EC4 formulas should not be employed for this series of experiments to predict the column capacities, because the strengths of both the concrete and the steel are over the stipulated limitations. In these experiments, the steel and concrete are both of high strength, and thus the point can be made that the present theoretical predictions for concrete-filled steel box columns are applicable for the various classes of strengths of steel and concrete used in construction.

The scatter of the present predictions versus each set of experiments are shown in Figs. 4-8, 4-9, and 4-10. Fig. 4-10 also contains scatters for predictions from the various design equations. The conclusion evident from these figures is that the present theoretical predictions are mostly below the experimental values, but not overly conservative.

Table 4.1 Comparison of the present theoretical predictions N_T with experiments [5]

1	2	3	4	5	6	7	8	9	10	11
Specimen	$b \times h$	b/t	σ_y	f_c'	σ_{cr}	N_u	N_T	N_t	N_T/N_u	N_t/N_u
NS1	180 × 180	60	294	33.6	291.1	1555	1554	1428.6	0.999	0.919
NS7	240 × 240	80	292	40.6	259.2	3095	2734	2548.8	0.883	0.824
NS13	300 × 300	100	281	44	187.3	4003	4040	3953.3	1.009	0.988
NS14	300 × 300	100	281	47	187.3	4253	4270	4182.8	1.003	0.983
NS15	300 × 300	100	281	47	187.3	4495	4270	4182.8	0.950	0.931
NS16	300 × 300	100	281	47	187.3	4658	4270	4182.8	0.917	0.898
Mean									0.960	0.924

Note: that the elastic modulus of steel is $E = 200\,\text{GPa}$; b, h = widths of steel sheet in each direction (mm), t- thickness of steel sheet (3 mm), σ_y = yielding stress of steel (MPa), f_c' = ultimate strength of concrete cylinder test (MPa), σ_{cr} = buckling load of steel plate (MPa), N_u = ultimate testing load of specimens (kN), N_T = ultimate predicted load by the present theory (kN), N_t = ultimate load predicted by Q. Q. Liang (kN).

Table 4.2 Comparison of the present theoretical predictions N_T with experiments [6]

1	2	3	4	5	6	7	8	9
Specimen	$b \times h$	b/t	σ_y	f_c'	σ_{cr}	N_u	N_T	N_T/N_u
HSSH1	100 × 100	20	750	NA	774.0	1644	1548	0.942
HSSH2	100 × 100	20	750	NA	774.0	1561	1548	0.992
HSS1	100 × 100	20	750	28	793.8	1836	1826	0.994
HSS2	100 × 100	20	750	28	793.8	1832	1826	0.997
HSS8	150 × 150	30	750	30	763.9	2868	2865	0.999
HSS9	150 × 150	30	750	30	763.9	2922	2865	0.980
HSS14	200 × 200	40	750	32	727.9	3710	4000	1.078
HSS15	200 × 200	40	750	32	727.9	3483	4000	1.148
Mean								1.016

Note: the Young's modulus of steel is 200 GPa; the symbols are same as in Table 4.1; the specimens of HSSH1 and HSSH2 are hollow section steel columns without concrete core.

Table 4.3 Geometric and material properties of test specimens [1]

1	2	3	4	5	6	7	8
Specimen	$B \times H$(mm)	$b \times h$(mm)	t(mm)	b/t	E(GPa)	σ_y(MPa)	f'_c(MPa)
C1-1	100.3 × 98.2	91.4 × 89.8	4.18	22	207	550	70.8
C1-2	101.5 × 100.6	93.1 × 92.2	4.18	22	207	550	70.8
C2-1	101.2 × 101.1	92.8 × 92.7	4.18	22	207	550	82.1
C2-2	100.7 × 100.4	92.3 × 92.0	4.18	22	207	550	82.1
C3	182.8 × 181.2	174.4 × 172.8	4.18	42	207	550	70.8
C4	181.8 × 180.4	173.4 × 172.0	4.18	42	207	550	82.1
C5-1	120.7 × 80.1	112.3 × 71.7	4.18	27	207	550	70.8
C5-2	119.3 × 80.6	110.9 × 72.2	4.18	27	207	550	70.8
C6-1	119.6 × 80.6	111.2 × 72.2	4.18	27	207	550	82.1
C6-2	120.5 × 80.6	112.1 × 72.2	4.18	27	207	550	82.1

Note: $B \times H$ = the dimension of section of columns, $b \times h$ = the dimension of section of concrete cores and widths of steel sheet in each direction; the other symbols have the same meaning as in Tables 4.1, 4.2.

Table 4.4 Comparison of the present theoretical predictions N_T with experimental results [1], EC 4, AISC, and ACI

1	2	3	4	5	6	7	8	9	10	11
Specimen	σ_{cr}	N_u	N_T	N_E	N_A	N_I	N_T/N_u	N_E/N_u	N_A/N_u	N_I/N_u
C1-1	572.0	1490	1366	1376	1291	1301	0.917	0.923	0.867	0.873
C1-2	572.0	1535	1403	1413	1325	1335	0.914	0.921	0.863	0.870
C2-1	572.0	1740	1488	1513	1409	1419	0.855	0.870	0.810	0.816
C2-2	572.0	1775	1475	1499	1397	1407	0.831	0.844	0.787	0.793
C3	543.8	3590	3393	3468	3171	3193	0.945	0.966	0.883	0.890
C4	543.8	4210	3653	3778	3429	3456	0.868	0.898	0.814	0.821
C5-1	564.9	1450	1354	1375	1282	1301	0.934	0.948	0.884	0.898
C5-2	564.9	1425	1347	1368	1276	1295	0.946	0.960	0.895	0.909
C6-1	564.9	1560	1427	1461	1353	1375	0.915	0.937	0.867	0.881
C6-2	564.9	1700	1436	1470	1361	1383	0.845	0.865	0.801	0.814
Mean							0.897	0.913	0.847	0.856

Note: EC4 = Eurocode 4, AISC = American Institute of Steel Construction, ACI = American Concrete Institute; The symbols σ_{cr}, N_u, N_T are the same as in Table 4.1. The symbols N_E, N_A, N_I denote the results calculated by design equations of EC4, AISC, and ACI receptively.

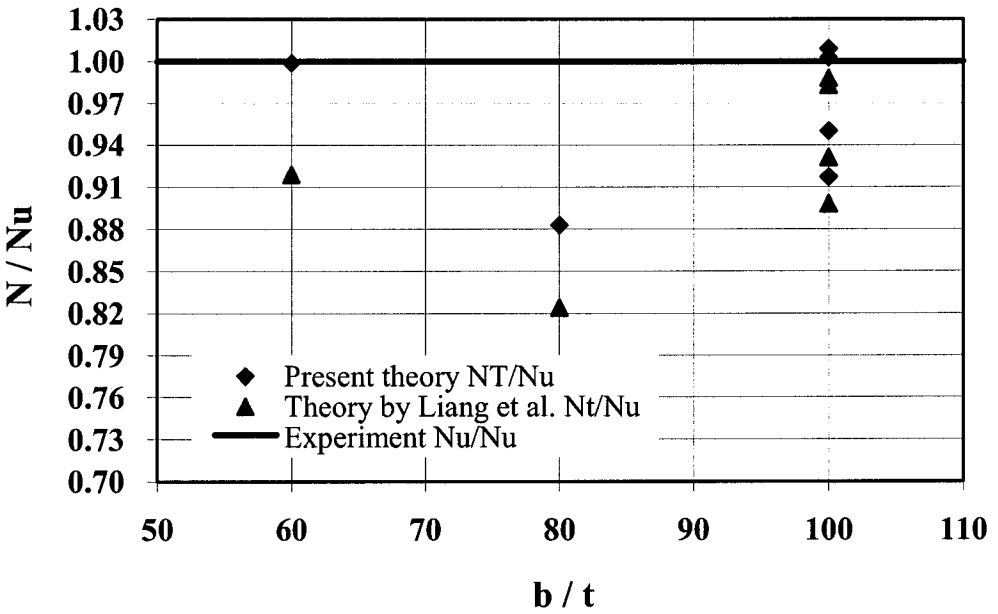

Fig. 4-8 Scatter for the present theoretical predictions vs. experiments in [5]

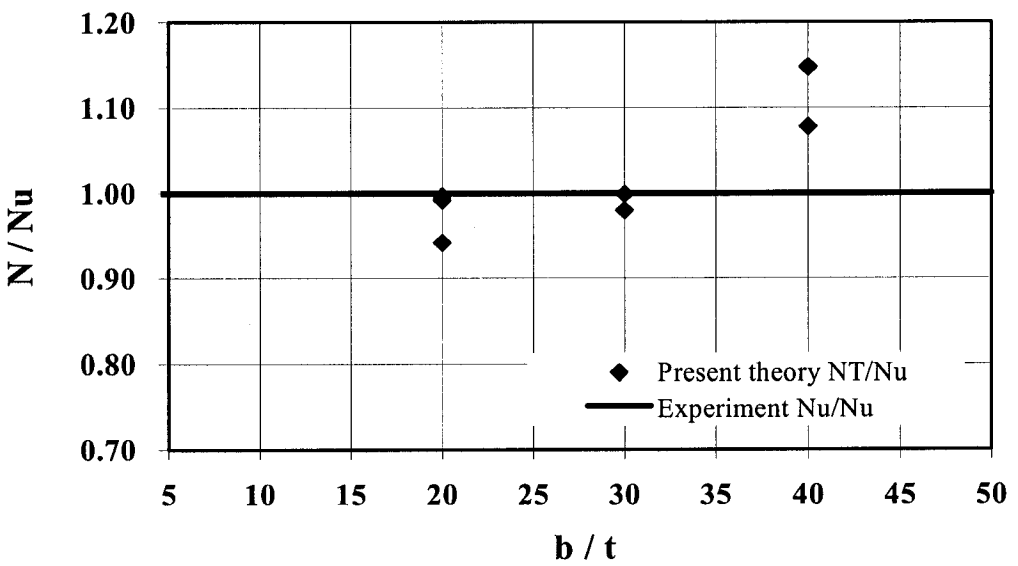

Fig. 4-9 Scatter for the present theoretical predictions vs. experiments in [6]

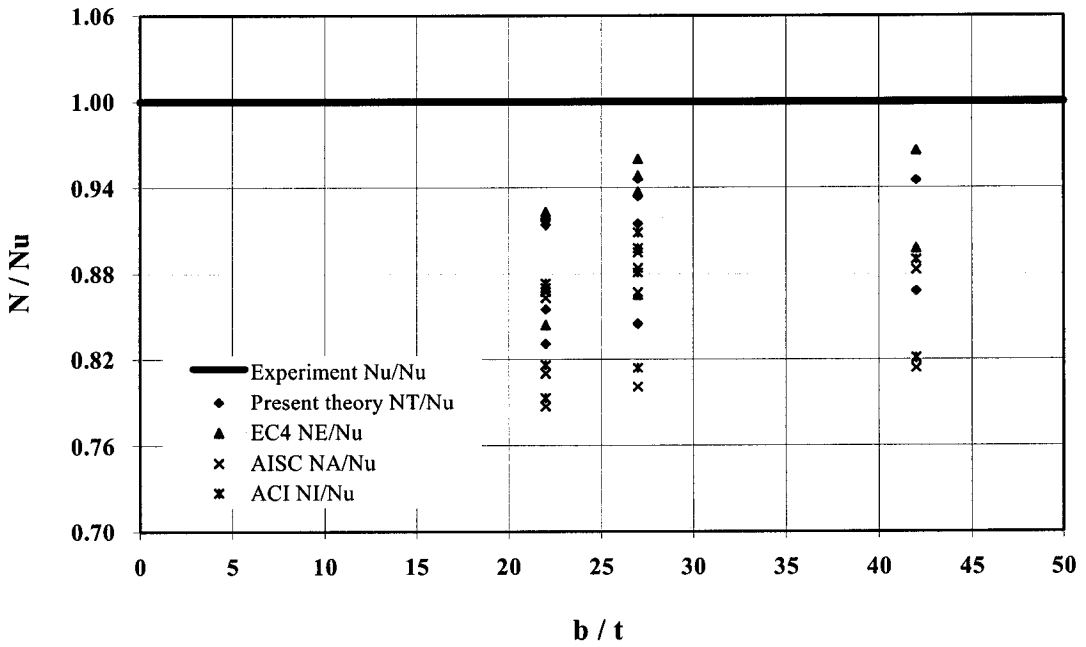

Fig. 4-10 Scatters for the present theory, EC4, AISC, and ACI vs. experiments in [1]

Chapter 5

Summary and Conclusions

5.1 Summary

Exact and semi-exact analyses have been performed to derive equations for obtaining bifurcation buckling loads, and wavelengths for infinitely long plates, stressed axially and resting on tensionless foundations. The plate material is considered to be linear elastic, as well as plastic. The elastic behaviour is modeled according to the standard linear relations employed for plate structures. The plastic behaviour is considered to be of the nonlinear strain-hardening type, employing the J_2 incremental as well as the J_2 deformation theories of plasticity. No bond is assumed to exist between the plate and the foundation. The foundation is thus unable to provide any tensile or frictional resistance. The compressive resistance from the foundation is assumed to be linearly proportional to plate deflection, with a constant modulus (modeling a one-way Wrinkler foundation). The plates are considered to be thin, and the usual kinematic assumptions for such plates are assumed to hold, regardless of the material behaviour. Two cases of boundary conditions are dealt with: (1) Plates simply supported along the two longitudinal (unloaded) edges, and (2) those with these edges clamped. Since the plates are considered infinitely long, the boundary conditions at infinity do not come into play, and therefore do not have any influence on the buckling loads or the wavelengths. The plates are assumed perfectly plane without any imperfections, and hence the buckling problem solved is that of a bifurcation type. In other words, the problem is posed as an eigenvalue problem. The eigenvalues are the bifurcation buckling loads, and the eigenmodes are the buckling modes. The analysis is exact for the simply supported case, but semi-exact for the clamped case. The main novelty of the investigation lies in including the plasticity effects, and applying the theoretical results to the practical problem of determining the buckling loads of concrete-filled steel box and HSS columns.

Chapter 1 gives a background on the general topic of plates resting on elastic foundations. Although there is considerable literature on this subject for the cases when the plate is bonded to the foundation, there are comparatively much less works on the subject when the plate is not bonded (or debonded) and the foundation is able to provide only the

compressive resistance. For the specific topic of buckling of plates on such tensionless foundations, the two most important works are by Shahwan [17] on elastic buckling of plates and of Seide [16] on plastic buckling. However, the work of Seide [16] dealt only with the elastic foundations with two-way actions. Hence the present work is the only one dealing with plastic buckling of plates on one-way elastic foundations.

The relevance of the present work to practical problems is also mentioned in this introductory chapter. The most immediate application, as mentioned above, is to the buckling of concrete-filled steel box and HSS columns. If the bonding between the steel plates and the concrete core is disregarded (as a safe and realistic assumption) then such problems fall into the category of the present study. The other important application, not pursued in this work, is to layered composite materials, in which delamination of a layer may be considered as a one-way elastic or plastic buckling.

The theoretical investigations in Chapter 2 are concerned with the elastic buckling of infinitely long plates on elastic foundations. The theory is developed first by adopting the equilibrium approach, and exact solutions are obtained for the buckling of plates simply supported on longitudinal edges and resting on tensionless foundations. Later, in this chapter, the method of virtual work is used to derive approximate equations for cases where separation of variables (used in the equilibrium method) may not be possible. The method of virtual work presented here is more general than the energy method, and includes the latter. The way the constitutive relations are specified makes the analysis applicable to the buckling of orthotropic elastic plates and also to plastic buckling of plates. This method is applied to derive the buckling conditions for a plate resting on tensionless foundations and clamped along the longitudinal edges. The solution gives the buckling load and the wavelengths in both the contact and no-contact zones. This solution is the same as that treated in Reference [17]. Although the results in Chapter 2 are not new, the method to obtain them is compact and new.

The results of Chapter 3, insofar as the plastic buckling of plates on tensionless foundations are concerned, are original to this thesis, and presented here for the first time. The theoretical development follows that of Chapter 2, but the plate material is allowed to be stressed beyond the yield into the strain-hardening plastic range. Accordingly, the constitutive relations of commonly used plasticity theories, namely the J_2 incremental and the J_2 deformation theories of plasticity are employed. Buckling equations are derived by the exact equilibrium method for plates simply supported on

longitudinal edges, and by the method of virtual work for plates clamped on these boundaries. The latter results are utilized in Chapter 4 for the buckling of concrete filled steel box columns. It should also be realized that although the J_2 incremental theory is the correct phenomenological theory of plasticity, its results are found to be highly imperfection sensitive in the case of buckling of plates. On the other hand, bifurcation results of the J_2 deformation theory are found quite acceptable, and in fact conservative, in comparison with experiments. Accordingly, it is only the bifurcation results of the J_2 deformation theory that are used in Chapter 4 for comparison with experiments on concrete-filled columns. Hutchinson has justified the use of the J_2 deformation theory in plastic buckling of plates [Ref. 28, p. 98]. He states that "... for a restricted range of deformations, J_2 deformation theory coincides with a physically acceptable incremental theory which develops a corner on its yield surface ... most of the results which have been obtained using J_2 deformation theory are *rigorously* (his italics) valid bifurcation predictions ...".

As the foundation modulus k increases, the contact wavelength decreases and the no-contact wavelength increases. As $k \rightarrow \infty$, i.e., as the foundation becomes rigid, the contact wavelength becomes zero and the bifurcation loads assume their maximum values as a logical consequence. For elastic buckling, it is found that the maximum enhancement over the case when no foundation is present ($k = 0$) is 33% for simple supports, and 42% for clamped supports along the longitudinal (unloaded) edges.

Compared to elastic buckling, the foundation effect on plastic buckling of plates is not as pronounced. For the stress-strain behaviour of the aluminum alloy 24S-T3 plate material, and the width to thickness ratio $b/t = 25$, the plastic bifurcation load for simply supported plates goes up by 7% from when $k = 0$ to when $k = \infty$. This ratio for the case of the clamped plate is 18%.

Although the analysis assumes infinitely long plates, the results seem to be applicable to plates with moderate aspect ratio. The study [4] points out that for a plate subjected to axial compression and resting on a tensionless foundation, its bifurcation load is little changed if the aspect ratio is greater than 1, especially if the foundation modulus is large. The results of the present theory are therefore applicable to most practical situations.

In Chapter 4, the results were compared with experimental results of other researchers, and also with empirical values from the design codes of different countries. The

comparison with three sets of test results on hollow or concrete-filled steel box columns, found that the values from the present theory to be 4% lower, 1% higher and 10% lower, respectively. These predicted values are in closer agreement with test results than the predictions of other researchers and those obtained by employing the empirical design code formulas.

5.2 Conclusions

In conclusion, one may reiterate the following points.

(1) The present study has performed, for the first time, exact and semi-exact analyses of (strain-hardening) plastic buckling of plates resting on one-way elastic foundations and subjected to uniform compressive forces in the longitudinal direction. The analysis is exact for plates simply supported on the long edges, and is semi-exact for plates clamped at these edges.

(2) The analytical predictions were compared with three independent sets of experimental data on buckling of concrete filled steel-box columns commonly used in engineering practice. The predictions of the present theory were in exceptionally good agreement with the diverse test results.

(3) Because of the good agreement between the present results and the test results, the present analytical results provide a rational basis for formulating comprehensive design criteria and equations applicable to high and low strength steel-box columns.

(4) The present exact and semi-exact analytical results may serve as bench mark results for validating finite element results.

5.3 Suggestions for future work

This type of investigation would be useful to other problems in practice, especially in aeronautical industry, such as the stability of other in-filled metal box columns (of say aluminum), delamination in sandwich plates, and delamination 'pop-up' in composite materials, etc.

For structural designer's convenience, one may also pursue the following tasks:

(1) Construct charts and tables to determine critical load coefficients from width to thickness ratios for steel plates, assuming rigid foundations.

(2) Modify the theoretical results for safe, economical, and comprehensive design equations.

References

[1] Liu, Dalin, Gho, Wie-Min, and Yuan, Jie, *Ultimate Capacity of High-strength Rectangular Concrete-filled Steel Hollow Section Stub Columns*, Journal of Constructional Steel Research, vol.59, 2003, pp.1499-1515.

[2] Roorda, John, *Buckles, Bulges and Blow-ups*, Applied Solid Mechanics, A. S. Tooth and J. Spence, eds., Elsevier Applied Science, New York, 1988, pp. 347-380.

[3] Chai, Herzl, Babcock, Charles D., and Knauss, Wolfgang G., *One Dimensional Modelling of Failure in Laminated Plates by Delamination Buckling*, International Journal of Solids Structures, vol.17, no.11, 1981, pp.1069-1083.

[4] Shahwan, Khaled W. and Anthony M. Waas, *Buckling, Postbuckling and Non-Self-Similar Decohesion along A Finite Interface of Uilaterally Constrained Delaminations in Composites*, PhD dissertation, Department of Aerospace. Engineering, The University of Michigan, Ann Arbor, Michigan, USA, 1995.

[5] Liang, Q. Q. and Uy, B., *Theoretical Study on the Post-local Buckling of Steel Plates in Concrete-filled Box Columns*, Computers and Structures, vol.75, 2000, pp. 479-490.

[6] Uy, B., *Strength of Short Concrete Filled High Strength Steel Box Columns*, Journal of Constructional Steel Research, vol.57, 2001, pp.113-134.

[7] Mursi, M. and Uy, B., *Strength of Concrete Filled Steel Box Columns Incorporating Interaction Buckling*, Journal of Structural Engineering, ASCE, vol.129, 2003, pp.626-638.

[8] Timoshenko, S. P. and Gere, J. M., *Theory of Elastic Stability*, McGraw-Hill, 1961.

[9] Bijlaard, P. P., *A Theory of Plastic Buckling with Its Application to Geophysics*, (published in May of 1938), Journal of the Aeronautical Science, vol.41, no.5, 1949, pp. 468-480.

[10] Bijlaard, P. P., *Theory and Tests on the Plastic Stability of Plates and Shells*, Journal of the Aeronautical Sciences, vol.16, no.9, 1949, pp. 529-541.

[11] Vlasov, V. Z. and Leont'ev, N. N., *Beams, Plates, and Shells on Elastic Foundations*, Translated from the Russian, Israel Program for Scientific Translations, Jerusalem, 1966, pp. 253-264.

[12] Weitsman, Y., *On the Unbonded Contact Between Plates and an Elastic Half Space*, Journal of Applied Mechanics, vol.36, no.2, Trans. of ASME, vol.91, Series E, June 1969, pp. 198-202.

[13] Weitsman, Y., *On Foundations That React in Compression Only*, Journal of Applied Mechanics, vol.37, Series E, no.4, 1970, pp.1019-1030.

[14] Celep, Zekai, *Rectangular Plates Resting on Tensionless Elastic Foundation*, Journal of Engineering Mechanics, vol.114, 1988, pp. 2083-2092.

[15] Seide, P., *Compressive Buckling of A Long Simply Supported Plate on An Elastic Foundation*, Journal of the Aeronautical Science, vol.25, 1958, pp. 382-384+394.

[16] Seide, P., *Plastic Compressive Buckling of Simply Supported Plates on Interior Elastic Supports*, Journal of the Aeronautical Sciences, vol.7, no.12, 1960, pp.921-925+950.

[17] Shahwan, Khaled W. and Anthony M. Waas, *Buckling of Unilaterally Constrained Infinite Plates*, Journal of Engineering Mechanics, vol.124, 1998, pp.127-136.

[18] Wright, H. D., *Buckling of Plates in Contact with A Rigid Medium*, The Structural Engineer, vol.71, no.12, 1993, pp. 209-214.

[19] Wright, H. D., *Local Stability of Filled and Encased Steel Sections*, Journal of Structural Engineering, vol.121, no.10, 1995, pp. 1382-1388.

[20] Wolfram Research, Inc., *Mathematica - A system for doing Mathematics,* Version 5.2, Champaign, Illinois, 2005.

[21] Hill, R., *The Mathematical Theory of Plasticity*, Oxford University Press, 1950.

[22] Berrada, K., *An Experimental Investigation of the Plastic Buckling of Aluminum Plates*, M.Eng. thesis, McGill University, 1985.

[23] Shanley, F. R., *The Column Paradox*, Journal of Aerospace Science, vol.13, 1946, 678 p.

[24] Shanley, F. R., *Inelastic Column Theory*, Journal of Aerospace Science, vol.14, 1947, pp. 261-267.

[25] Shrivastava, S. C., *Inelastic Buckling of Plates Including Shear Effects*, International Journal of Solids and Structures, vol.15, 1979, pp. 567-575.

[26] Ramberg, W. and Osgood, W. R., *Description of Stress-Strain Curves By Three Parameters*, NACA, Tech. Note, no.902, 1946, pp.1-13.

[27] Chajes, Alexander, *Principles of Structural Stability Theory*, Waveland Press, 1993.

[28] Hutchinson, J. W., *Plastic Buckling*, Advances in Applied Mechanics, C.-S., Yih, ed., v.14, 1974, pp. 67-144.